NRL REPORT NO. R-3280

[redacted]

FR-3280

PROPOSED CONSTANT TRUE BEARING HOMING SYSTEM FOR SKYLARK

NAVAL RESEARCH LABORATORY

WASHINGTON, D.C.

~~CONFIDENTIAL~~

NRL REPORT NO. R-3280

PROPOSED CONSTANT TRUE BEARING HOMING SYSTEM FOR SKYLARK

Peter Waterman, Carroll L. Key
and Charles H. Dodge

April 16, 1948

Approved by:

Dr. R. M. Page, Superintendent, Radio Division III

NAVAL RESEARCH LABORATORY
CAPTAIN H. A. SCHADE, USN, DIRECTOR
WASHINGTON, D.C.

DISTRIBUTION

	Copy No.
Guided Missile Committee, RDB, Wash., D. C.	A (1-2)
Ch. of Staff, USAF, Pentagon, Wash., D. C., Attn: DCS/M, MRD-4	" (3-6)
CG, AMC, Wright-Patterson Air Force Base, Dayton, Ohio, Attn: MCIDXD	" (7-29)
CG, Air Univ., Maxwell Field, Ala., Attn: Air Univ. Lib.	" (30)
BuAer, Wash., D. C., Attn: TD-4	" (31-36)
BuOrd, Wash., D. C., Attn: Re-9	" (37-40)
BuShips, Wash., D. C., Attn: Code 633	" (41-43)
Ch/GMBranch, Technical Command, Army Chem. Center, Md.	" (44)
CG, APG, Md., Attn: Ballistics Res. Lab.	" (45)
CG, Eglin Field, Fla., Attn: First Exp., Guided Missiles Group	" (46)
CO, AAS, Fort Bliss, Texas	" (47)
CO, Frankford Arsenal, Phila., Pa., Attn: Fire Control Design Div.	" (48)
Comdr., MAMC, Phila., Pa.	" (49)
CO, NADS, Johnsville, Pa.	" (50)
CO, ONR, San Francisco, Calif.	" (51)
CO, SCEL, Ft. Monmouth, N. J.	" (52)
CO, NAMTC, Pt. Mugu, Calif.	" (53)
CO, NOTS, Inyokern, Calif., P. O. China Lake, Calif.	" (54)
CO, Holloman Air Force Base, Alamogordo, N. M.	" (55)
Dir., DTMB, Wash., D. C., Attn: Aerodynamics Div.	" (56)
Dir., NACA, Wash., D. C., Attn: Mr. C. H. Helms	" (57-60)
Dir., NRL, Wash., D. C.	" (61-62)
Dir., Spec. Devices Center, ONR, Sands Point, L. I., N. Y., Attn: TID	" (63)
First Anti-Aircraft Artillery GM Btn., WSPG, Las Cruces, N. M.	" (64)
Supt., PG School, U. S. Naval Academy, Annapolis, Md.	" (65)
Dept. of the Army, Office of the Ch. of Ord., Pentagon, Wash., D. C. Attn: ORDTU	" (66-67)
OinC, NOEU, Nat'l BuStds., Wash., D. C.	" (68)
OinC, NOL, White Oaks, Md., Wash., D. C., Attn: Dr. R. J. Seeger	" (69-70)
OinC, Ord. Res. & Dev. Div. Sub-Office (Rocket) Ft. Bliss, Texas	" (71)
CNO, Wash., D. C., Attn: Op-57	" (72)
Watson Labs., AMC, Eatontown, N. J.	" (73)
Watson Labs., AMC, Cambridge Field Sta., Cambridge, Mass., Attn: Dr. Marcus O'Day	" (74)
CG, Army Ground Forces, Ft. Monroe, Va., Attn: Ch/Dev. Sect. GNDEV-9	" (75)
ONR, c/o Lib. of Congress, Science & Technology Project, Wash., D. C.	" (76-78)
Ch/Res. and Eng. Div., Off. Ch. Chem. Corps, Army Chem. Center, Md.	" (79)
CO, NAOTS, Chincoteague, Va.	" (80)
CG, WSPG, Las Cruces, N. M.	" (81)
DCO for APL, JHU, Silver Spring, Md., Attn: Dr. Dwight E. Gray	C (1-3)
BAC, Niagara Falls, N. Y., Attn: Mr. R. H. Stanley & Mr. B. Hamlin	" (4)
BTL, Whippany, N. J., Attn: Mr. W. C. Tinus	" (5)
INSMAT for Bendix Av. Corp., Detroit, Mich., Attn: Dr. Harner Selvidge	" (6)
Boeing Aircraft Corp., Seattle, Wash., Attn: Mr. R. H. Nelson	" (7)
DCO for C-V Air. Corp., Daingerfield, Texas, Attn: Mr. J. E. Arnold	" (8)
BAR for C-V Air. Corp., San Diego, Calif., Attn: Mr. A. W. Abels	" (9)
DCO for Cornell Aero. Lab., Buffalo, N. Y., Attn: Mr. W. M. Duke	" (10)
BAR for Curtiss-Wright Corp., Columbus, Ohio, Attn: Mr. Bruce Eaton	" (11)
BAR for Douglas Aircraft Co., El Segundo, Calif., Attn: Mr. E. H. Heinemann	" (12)
Douglas Aircraft Co., Santa Monica, Calif., Attn: Mr. A. E. Raymond, (Project RAND) and Mr. E. F. Burton	" (13-14)
INSORD for Eastman Kodak Co., Rochester, N. Y., Attn: Dr. H. Trotter	" (15)

		Copy No.
Fairchild Eng. and Air. Corp., NEPA Div., Oak Ridge, Tenn., Attn: Mr. A. Kalitisky, Ch. Engr.	C	(16)
RIC-BuAer for Fairchild Eng. and Air. Corp., Farmingdale, L. I., N. Y., Attn: Mr. J. A. Slonim	"	(17)
INSMAT for Franklin Inst. Labs. for Res. and Dev., Phila., Pa., Attn: Mr. R. H. McClarren	"	(18)
AOLO for G. E. Co., Schenectady, N. Y., Project HERMES, Attn: Mr. C. K. Bauer	"	(19)
G. E. Co., Schenectady, N. Y., c/o Inspector of Machinery, USN	"	(20)
G. E. Co., Av. Div., Schenectady, N. Y., Attn: Mr. S. A. Schuler, Jr. and Mr. Phillip Class	"	(21)
BAR for Glenn L. Martin Co., Baltimore, Md., Attn: Miss. T. R. McNabb	"	(22)
INSMAT, Chicago for Globe Corp., Joliet, Ill., Attn: Mr. J. A. Weagle	"	(23)
BAR for Grumman Air. Engr. Corp., Bethpage, L. I., N. Y., Attn: Mr. Wm. T. Schwendler	"	(24)
District Chief for CIT, Jet Propulsion Lab., Pasadena, Calif., Attn: Mr. L. G. Dunn	"	(25-26)
INSMAT, Brooklyn for Kellex Corp., N. Y., N. Y.	"	(27)
NORTLO for Chm., MIT, GMC, Project Meteor Office, Cambridge, Mass., Attn: GM Lib.	"	(28-29)
BAR for McDonnell Aircraft Corp., St. Louis, Mo., Attn: Mr. W. P. Montgomery	"	(30)
North Am. Aviation, Inc., Los Angeles, Calif., Attn: Mr. D. H. Mason	"	(31)
Northrop Aircraft Inc., Hawthorne, Calif., Attn: Mr. S. E. Weaver	"	(32)
DCO, Newark for Princeton Univ., Princeton, N. J., Attn: Mr. Harry Ashworth, Sr.	"	(33)
CO, ONR Branch Office, Brooklyn for Princeton Univ., Princeton, N. J., Attn: Project SQUID	"	(34-36)
INSMAT for Radio Corp. of Am., Camden, N. J., Attn: Mr. T. T. Eaton	"	(37)
BAR, Burbank for Radioplane Corp., Van Nuys, Calif., Attn: Mr. F. Smith	"	(38)
INSMAT, Boston for Raytheon Mfgr. Co., Waltham, Mass., Attn: Mrs. H. L. Thomas	"	(39)
INSMAT, Brooklyn for Reeves Instrument Corp., N. Y., N. Y.	"	(40)
Ryan Aero. Co., Lindberg Field, San Diego, Calif., Attn: Mr. H. A. Sutton	"	(41)
INSMAT, Brooklyn for Sperry Gyroscope Co, Inc., Great Neck, L. I., N. Y.	"	(42)
BAR for U. A. Corp., Chance Vought Aircraft Div., Stratford, Conn. Attn: Mr. P. S. Baker	"	(43)
BAR for U. S. Corp., Res. Dept., E. Hartford, Conn., Attn: Mr. J. G. Lee	"	(44)
Univ. of Mich., Aero Res. Center, Willow Run Airport, Ypsilanti, Mich., Attn: Mr. R. F. May	"	(45)
BAR, Pasadena for Univ. of S. Cal., Naval Res. Proj., Los Angeles, Calif., Attn: Dr. R. T. De Vault	"	(46)
DCO for Univ. of Texas, Defense Res. Lab., Austin, Texas, Attn: Dr. C. P. Boner	"	(47)
Lockheed Aircraft Corp., Burbank, Calif., Attn: Mr. H. L. Hibbard	"	(48)
Univ. of Chicago.. Ord. Res., Chicago, Ill.	"	(49)
BAR, Brooklyn for Airborne Instr. Lab., Mineola, L. I., N. Y., Attn: Mr. Walter Tolles	DG	(1)
Belmont Radio Corp., Chicago, Ill., Attn: Mr. Harold C. Mattes	"	(2)
BARR for Bendix Aviation Corp., Teterboro, N. J., Attn: Mr. R. C. Sylvander	"	(3)
DCO for Bendix Av. Corp., N. Hollywood, Attn: Mr. R. M. Russell	"	(4)
Bendix Aviation Radio Div., Baltimore, Md., Attn: Mr. A. C. Omberg	"	(5)
Buehler & Co., Chicago, Ill., Attn: Mr. Jack M. Roehn	"	(6)
Ch. of Staff, USAF, Pentagon, Attn: DCS/M, AFMRD-5A	"	(7)
BAR for Consolidated-Vultee Aircraft Corp., San Diego, Calif., Attn: Mr. C. J. Breitwieser	"	(8)
INSMAT, Chicago for Collins Radio Co., Cedar Rapids, Iowa	"	(9)
Cornell Univ., Ithaca, N. Y., Attn: Mr. Wm. C. Ballard, Jr.	"	(10)
Dir., USNEL, San Diego, Calif.	"	(11)
INSMAT, Boston for Doelcam Corp., West Newton, Mass., Attn: Mr. J. J. Wilson	"	(12)
Electro Mechanical Res., Ridge Field, Conn., Attn: Mr. Charles B. Aiken	"	(13)
Eltron, Inc., Jackson, Mich., Attn: Mr. D. B. Mason	"	(14)
Fairchild Camera and Instr. Corp., Jamaica, L. I., N. Y., Attn: Mr. Avery Lockner	"	(15)
DCO for Farnsworth Television & Radio Co., Ft. Wayne, Ind., Attn: Mr. J. D. Schantz	"	(16)
Federal Telephone & Radio Corp., Newark 4, N. J., Attn: Mr. E. N. Wendell	"	(17)
Galvin Mfg. Corp., Chicago, Ill., Attn: Mr. G. R. MacDonald	"	(18)

	Copy No.
INSMAT for G. E. Co., Syracuse, N. Y., Attn: Mr. W. Hafstrom	DG (19)
Gilfillan Corp., Los Angeles, Calif., Attn: Mr. G. H. Miles	" (20)
G. M. Giannini and Co., Inc., Pasadena, Calif.	" (21)
Goodyear Aircraft Corp., Plant "B", Akron, Ohio, Attn: Mr. A. J. Peterson	" (22)
INSMAT, Brooklyn for Hillyer Eng. Co., N. Y., N. Y., Attn: Mr. Curtiss Hillyer	" (23)
Hughes Aircraft Co., Culver City, Calif., Attn: Mr. D. H. Evans	" (24)
INSMAT, Brooklyn for Kearfott Co., Inc., N. Y., N. Y.	" (25)
Lear, Inc., Grand Rapids, Mich., Attn: Mr. R. M. Mock	" (26)
Mfg. Machine and Tool Co., Mt. Vernon, N. Y., Attn: Mr. Jacob Kloppinger, U. P.	" (27)
Minneapolis-Honeywell Mfgr. Co., Minneapolis, Minn. Attn: Mr. W. J. McGoldrick, Vice Pres.	" (28)
DCO, INSMAT, Newark for M. W. Kellogg Co., Jersey City, N. J. Attn: Dr. G. H. Messerly	" (29)
Ohio State Univ., Columbus, Ohio, Attn: Mr. Thomas E. Davis, Staff Asst.	" (30)
Haller, Raymond and Brown, State College, Pa., Attn: Dr. R. C. Raymond, Pres.	" (31)
CO, ONR Branch Office, Brooklyn for Radio Corp. of Am. Labs., Princeton, N. J., Attn: Mr. A. W. Vance	" (32)
Republic Av. Corp., Farmingdale, L. I., N. Y., Attn: Dr. Wm. O'Donnell	" (33)
OCSigO, Eng. and Tech. Ser., Engr. Div., Pentagon, Washington, D. C.	" (34)
L. N. Schwein Eng. Co., Los Angeles, Calif., Attn: Mr. L. N. Schwein	" (35)
SNLO, USNELO, Ft. Monmouth, N. J.	" (36)
INSMAT, Brooklyn for Servo Corp. of Am., Lindenhurst, L. I., N. Y., Attn: Mr. H. Blackstone, Pres.	" (37)
BAR, Brooklyn for Square D. Co., Elmhurst, N. Y., Attn: Mr. V. E. Carbonara	" (38)
DCO, MIT, Cambridge for Submarine Signal Co., Boston, Mass., Attn: Mr. Edgar Horton	" (39)
Summers Gyroscope Co., Santa Monica, Calif., Attn: Mr. Tom Summers, Jr.	" (40)
INSMAT, Brooklyn for Sylvania Electric Products, Flushing, L. I., N. Y., Attn: Dr. Robert Bowie	" (41)
Teleregister Corp., N. Y., N. Y., Attn: Mr. M. L. Haselton	" (42)
Univ. of Pittsburgh, Pittsburgh, Pa., Attn: Mr. E. A. Holbrook, Dean	" (44)
DCO for Univ. of Va., Charlottesville, Va., Attn: Dr. J. W. Beams	" (45)
Washington Univ., Clayton, Mo., Attn: Dr. R. C. Spencer	" (46)
Westinghouse Electric Corp., Pittsburgh, Pa., Attn: Mr. F. W. Godsey, Jr., Mgr.	" (47)
Dir. of Specialty Products Dev., Whippany Radio Lab., Whippany, N. J., Attn: Mr. R. E. Poole	" (48)
Zenith Radio Corp., Chicago, Ill., Attn: Mr. Hugh Robertson, Exec. Vice Pres.	" (49)

CONTENTS

ABSTRACT

A terminal guidance system of a constant true bearing type for missile guidance is discussed with direct reference to the Skylark program. Consideration involving the control loop, passive target tracking device, launching dispersion, interaction, and the airframe autopilot are given which result in a system proposal.

PROBLEM STATUS

This is an interim report on this problem.

AUTHORIZATION

NRL Problem No. R05-29 (BuAer-313).

PROPOSED CONSTANT TRUE BEARING HOMING SYSTEM FOR SKYLARK

INTRODUCTION

A constant true bearing trajectory is one in which the direction of the bearing line from the missile to the target remains fixed in space. For a target flying a straight line at a constant speed, the resulting missile trajectory is a straight line. The missile is required to change heading to maintain the correct course only when the target changes either heading or speed.

If the target (Figure 1) at time "O" is flying at constant speed toward interception point D_1 and the missile at that time is also flying at constant speed toward D_1, the bearing line is at a constant angle β in space. The missile is flying a constant true bearing course. If at time "x" the target changes heading, the missile must also change heading in order to keep the true bearing constant. It must turn so as to maintain β constant. Interception will occur at D_2. A system to cause the missile to function in this manner is proposed in this paper.

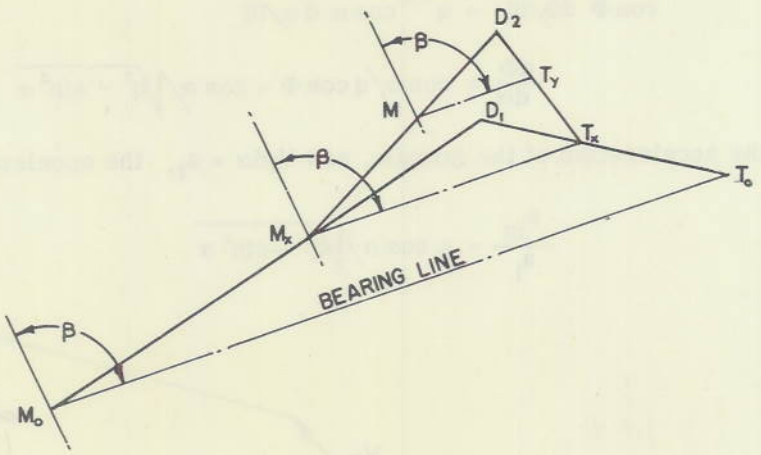

Figure 1

Dr. L. J. Chu of the Massachusetts Institute of Technology showed, in his report on homing, that the constant true bearing homing course is the ideal homing course. In brief, the proof is as follows: At any instant a missile is limited in the positions to which it can fly by its maximum rate of turn. If the missile is at M_O and pointed toward D_O it cannot fly into the area shaded in Figure 2. The area to which the missile can fly is rapidly reduced

as the range to the target is reduced. The area is proportional to the fourth power of the distance to the target. Hence, it is desirable to align the missile axis with the instantaneous interception point as early as possible in homing flight, in order to allow the missile further to alter its course to correct for any change in the interception point. That is, the missile should point toward what would be an interception point were the target at that time to continue flying in a tangent straight line. This is a constant true bearing trajectory.

Of interest in the development of missiles and control systems is a study of what turning rate is demanded of the missile in order to follow any particular trajectory. Pure pursuit and deviated pursuit trajectories call for high or infinite rates of turn at the end of the flight. Proportional navigation (partial navigation) has a rate of turn which varies with the parameters of the system, but is in any case higher than that required for the constant true bearing system. It may be seen from Figure 3 that, in order to keep the true bearing angle constant

$$V_m \sin \Phi = V_t \sin \alpha \tag{1}$$

letting "q" be the velocity ratio

$$q = V_m / V_t \tag{2}$$

then $$\sin \Phi = \frac{1}{q} (\sin \alpha)$$

and $$\cos \Phi = \sqrt{1 - \sin^2 \alpha / q^2} \tag{3}$$

Taking the derivative of equation (3)

$$\cos \Phi \, d\Phi / dt = q^{-1} \cos \alpha \, d\alpha / dt$$

$$\frac{d\Phi}{d\alpha} = \cos \alpha / q \cos \Phi = \cos \alpha / \sqrt{q^2 - \sin^2 \alpha} \tag{4}$$

but $V_m \, d\Phi = a_m$, the acceleration of the missile, and $V_t d\alpha = a_t$, the acceleration of the target, so:

$$\frac{a_m}{a_t} = q \cos \alpha / \sqrt{q^2 - \sin^2 \alpha} \tag{5}$$

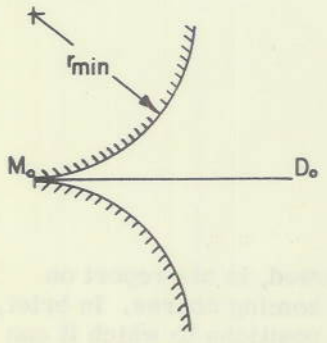

Figure 2

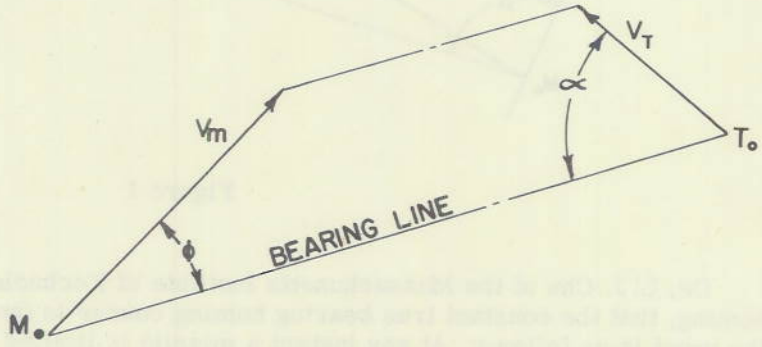

Figure 3

It is apparent that the maximum value of the right hand side of the equation is 1, when $\alpha = 0^0$ and a minimum 0 when $\alpha = 90^0$. It is evident that the maximum acceleration of the missile is never greater than that of the target. For any other type of homing course, this demand will be greater. In fact, if some computer were employed to compute a homing trajectory, the ideal computer would be the one which would cause the missile to fly a constant true bearing course.

The development of a control system or simple computing device involves a study of the interrelations among the various portions of the system. A discussion of some of the considerations involved in such a design follows.

DESIGN CHARACTERISTICS FOR THE MISSILE-AUTOPILOT COMBINATION

It is important to be able to assign definite transmission characteristics to all portions of a complex system. The autopilot has two interrelated jobs to do in the overall problem.

(a) It must stabilize the airframe so that external disturbances will not throw the missile out of control.

(b) It must operate on control error signals in some way to cause the airframe to change heading in a consistent manner.

For the design of this system the autopilot missile combination has been specified as one to act as an integrator of the input control signals. This requires satisfactory design of the autopilot so that rate of turn is proportional to the error signal from the control system. The missile is to be allowed to fly with a small residual angle of attack, that is, the axis of the missile does not necessarily have to coincide with the tangent to the missile trajectory.

For the system to operate without elaborate commutation system it is necessary that the missile be roll stabilized and, further, it is desirable that any roll present have a natural frequency greater than the frequencies passed by the control system.

DESIGN CHARACTERISTICS FOR THE RADAR TRACKING LOOP

Since the constant true bearing system attempts to reduce the rate of change of tracking angle to zero, various types of tracking devices can be employed. Some applicable tracking devices are:

(1) Conventional conical scan radars, either active or passive, using either CW or pulse transmission.

(2) Directionally directed, simultaneous lobe comparison radars, either active or passive, CW or pulse transmission.

(3) Radars depending on phase comparison of multilobe antenna patterns with the phase comparison occuring at either RF, IF or video frequencies.

(4) High speed lobing radars.

Since the actual radar characteristics involved do not constitute a part of this study, it has for simplicity been assumed the use of a conical scan passive radar, although this study is applicable to a system using any of the above named radars.

DESIGN CHARACTERISTICS FOR THE CONSTANT BEARING CONTROL SYSTEM

It has been shown that all that is required to establish a constant true bearing homing system is to keep the angle of the bearing line from the missile to the target, measured relative to any line fixed in space, a constant. One way to accomplish this is to measure the rate of change of this angle and to utilize this signal to operate the directional control system of the missile in such a manner as to keep the rate of change of bearing angle zero.

This development is carried out with separate systems for yaw and pitch, the two systems being essentially identical. The following discussion will be concerned with a single system, one which will be duplicated in the other coordinate.

Since there is a limit to the minimum rate of change of bearing which a system can measure and because there is an ever present possibility that, due to radar tracking operation or due to target propagation difficulties, there may be momentary lapses in control information, it is desirable that the loop have some memory, or integration characteristics. This memory characteristic can be used to maintain a rate of turn although the control signal proportional to the rate of change of the bearing line may be zero. This allows reduced error in intercepting targets flying other than straight line courses.

The physical system under consideration can be further delineated as follows:
On the radar tracking head, a rate gyro is mounted in such a way as to measure the rate of change of heading of the tracking head. The output of the gyro will be proportional to the rate of change of true bearing, which can be written

$$k E_o = \dot{\beta} \text{ or } \frac{p}{\omega_1} \beta = E_o \qquad (6)$$

where $p\beta = \frac{d\beta}{dt} = \dot{\beta}$

and β = angle between true bearing line and a reference line

E_o = the voltage output

$p = d/dt$

and ω_1 = a gain constant associated with the rate gyro.

This signal will be amplified and then fed into a memory circuit (integrator). The output from the memory circuit will be fed into the autopilot as an error signal to vary the angle of the flaps. The missile will respond to this error signal in the same manner as it responds to signals from the autopilot due to external disturbances.

DESIGN CHARACTERISTICS FOR THE OWN SHIP'S ANGLE LOOP

Inasmuch as the radar dish is mounted in the missile, any change in missile attitude would cause the antenna dish to rotate with the missile if correction were not made. This would place an excessive burden on the radar tracking loop which would have to track out missile motion as well as perform its normal function of tracking out target motion. It is desirable, therefore, to make the gimble drive respond to changes in missile heading and to subtract missile heading changes out of the antenna. This is, in effect, stabilizing the antenna in space, and will be done with the own ship's angle loop.

The necessity of the own ship's angle correction servo loop is further apparent from consideration of the fact that without it corrections in missile heading are reflected as changes in antenna position in the same direction as the changes in true bearing causing that correction. As it may be assumed that the action of the radar tracking loop is not instantaneous and that the control circuits in the missile have gain greater than unity, the action of the system would be regenerative, hence unstable.

The own ship's angle loop will be a loop similar to that used to remove roll and pitch in fire control systems aboard ship. This simple system can be made to follow the missile motions with high precision.

BANDPASS CONSIDERATIONS

For the analysis of this system (Figure 4) operational methods shall be used in which frequency response characteristics for mechanical parts are expressed in a manner similar to that used conventionally for electrical parts. Hence, the problem resolves itself into a

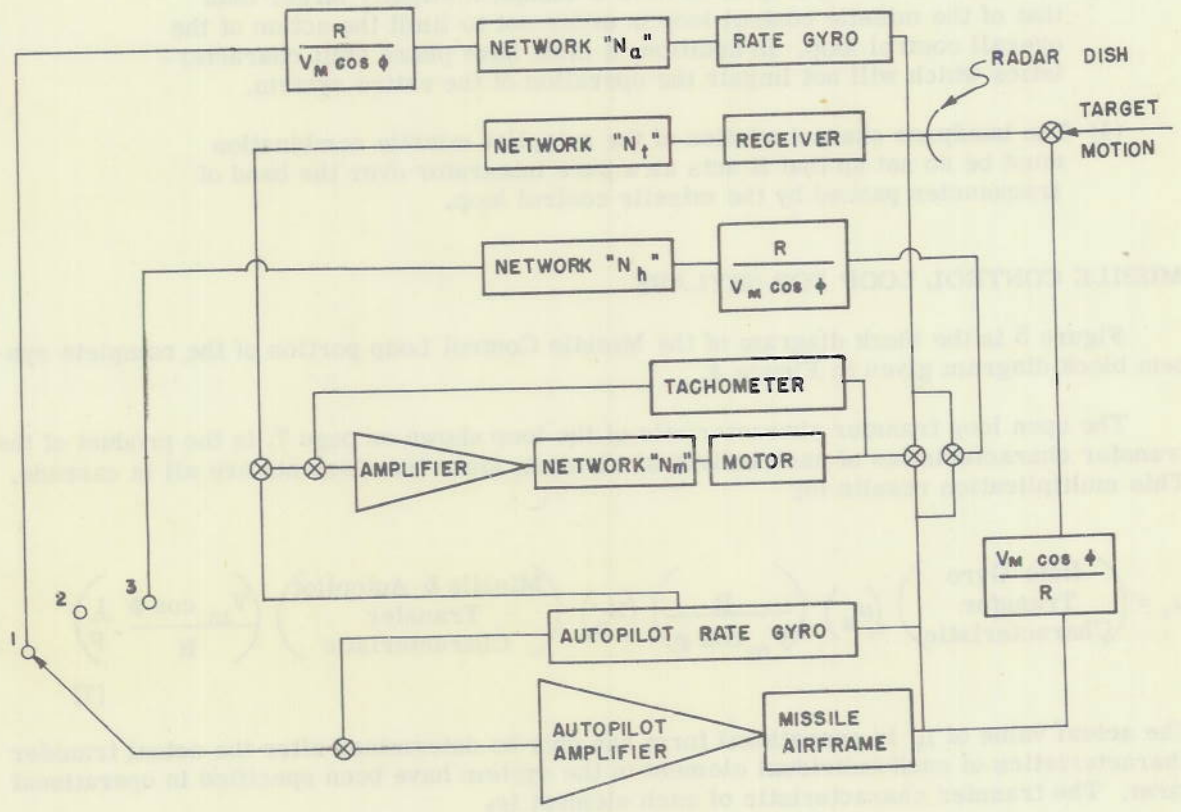

Figure 4

problem of network analysis and feedback amplifier design. As in the conventional amplifier design, the effect of noise may be minimized by restricting the bandpass of the system to that necessary to pass the input signal to the accuracy desired. Therefore, the design of the components of this system presupposes the knowledge of the input signals and the accuracy

required. Studies of the frequency spectrum of the input signal are made to determine the minimum bandpass required to pass these signals with sufficient accuracy.

At this point no statements can be made as to the actual bandpass requirements for the various loops since no missile characteristics are yet assumed, but statements can be made concerning the relationships existing among them.

(1) The bandwidth of the missile control system, including the missile and autopilot, must be sufficient to cause the missile to follow the desired trajectory with accuracy consistent with the tactical requirements.

(2) The own ship's motion loop must have a bandpass considerably wider than that of the missile control loop in order to subtract accurately the missile motion due to the trajectory from the antenna. In addition, the bandpass must be wide enough to subtract out missile motion due to other causes, such as gust conditions, etc.

(3) The radar tracking loop must have a bandpass slightly larger than that of the missile control loop in order not to limit the action of the overall control loop. In addition, it must have phase shift characteristics which will not impair the operation of the entire system.

(4) The bandpass characteristics of the autopilot missile combination must be so set up that it acts as a pure integrator over the band of frequencies passed by the missile control loop.

MISSILE CONTROL LOOP FOR SKYLARK

Figure 5 is the block diagram of the Missile Control Loop portion of the complete system block diagram given in Figure 4.

The open loop transfer characteristic of the loop shown on page 7, is the product of the transfer characteristics of each individual element, since the elements are all in cascade. This multiplication results in:

$$\mu_1 = \left(\begin{array}{c}\text{Rate Gyro}\\ \text{Transfer}\\ \text{Characteristic}\end{array}\right)\left(\mu_a\right)\left(\frac{R}{V_m \cos\Phi}\right)\left(N_a\right)\left(\begin{array}{c}\text{Missile \& Autopilot}\\ \text{Transfer}\\ \text{Characteristic}\end{array}\right)\left(\frac{V_m \cos\Phi}{R}\,\frac{1}{p}\right) \tag{7}$$

The actual value of μ_1 in operational form can only be determined after the actual transfer characteristics of each individual element in the system have been specified in operational form. The transfer characteristic of each element is:

(a) Rate Gyro

The action of a rate gyro is to give an electrical output directly proportional to the time rate of change of the angle it is measuring. As in all physical devices, this characteristic is true only under limited conditions determined by the physical characteristics of the unit. Since the amplitude of output will drop at frequencies higher that the resonant frequency, the

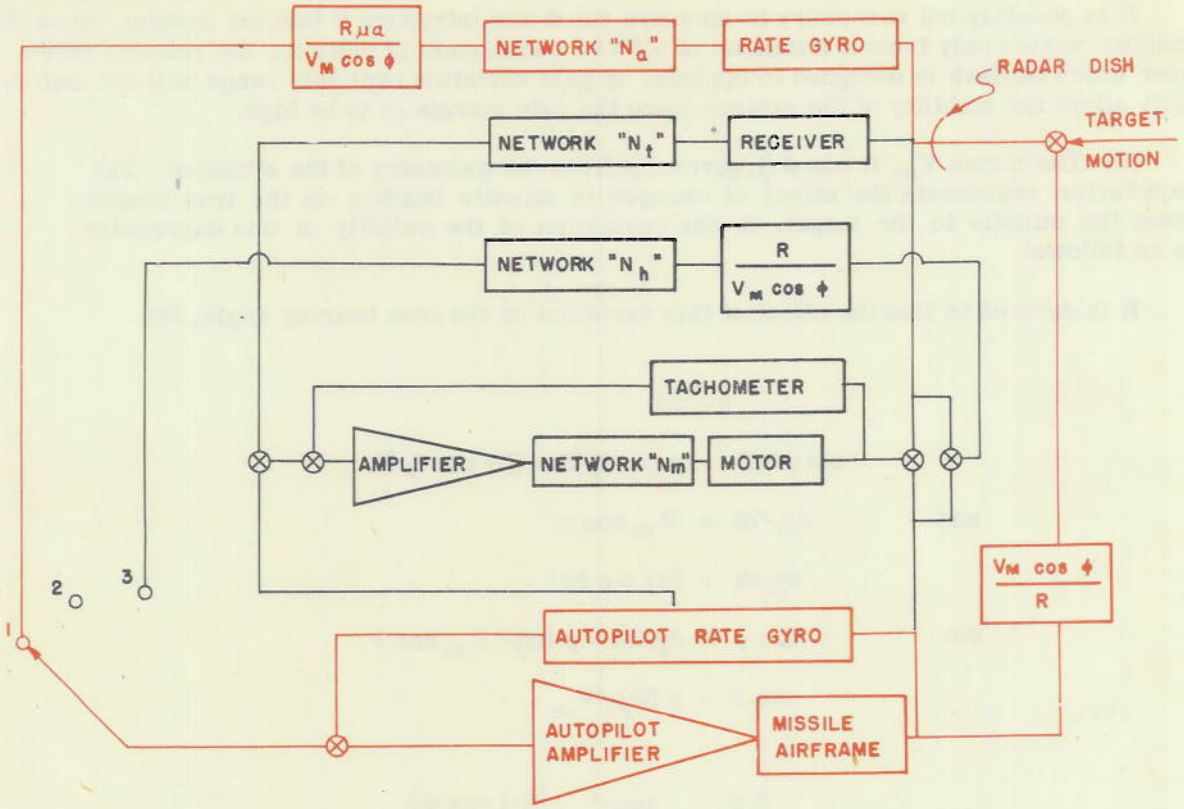

Figure 5

resonant frequency of the rate gyro should be set so that it is higher than the frequency of gain crossover of the constant true bearing control loop. For purposes of analysis, the transfer characteristics of the rate gyro to be used in this application is assumed to be p/ω_t over the bandpass of the Missile Control Loop. A more detailed analysis is given in Appendix I.

Academically the presence of a rate gyro mounted on the rear of the tracking radar dish may not be absolutely necessary. Instead, the output of the receiver (which indicates changes in the true bearing from the missile to the target) could be utilized. The use of the receiver as an error indicating device for control, however, would require equalization of the tracking loop to make the receiver output directly proportional to either β or $\dot{\beta}$, thus necessitating design of the receiver for two uses, both tracking the target and missile control. This would restrict freedom to set the receiver loop characteristics to those which would give optimum signal to noise ratio and tracking accuracy.

(b) μ_a represents the gain of a conventional amplifier which is linear over all frequencies that we are interested in passing.

(c) The term $R/\cos\Phi$ is introduced into the amplifier described in (b) as a gain control voltage, to make the gain proportional to $R/\cos\Phi$. The range portion of this term will be generated in the missile receiver. The $\cos\Phi$ can be measured inside the missile by a differential yoke connected across the differential connecting the antenna to the missile, (i.e., from the antenna to the body of the missile.)

It is possibly not necessary to measure $\cos\Phi$ and introduce it into the system, since this function varies only from a minimum of 0.86 to a maximum of unity for the velocity ratios over which Skylark is designed to operate. A gain variation over this range will not materially affect the stability of the system since the gain margin is to be high.

(d) The terms $V_m/R \cos\phi (1/p)$ results from the geometry of the situation. The expression represents the effect of changes in missile heading on the true bearing from the missile to the target. A demonstration of the validity of this expression is as follows:

It is desired to find the effect of this variation on the true bearing angle. Set

$$y = f(t)$$

$$\sin(-\Delta\beta) = y \cos\Phi/R = f(t) \cos\Phi/R$$

and

$$dx/dt = V_m \cos\gamma$$

$$dy/dt = \dot{f}(t) = p\, f(t)$$

but

$$\tan\gamma = dy/dx = p\, f(t)/V_m \cos\gamma$$

$$\sin\gamma = p\, f(t)/V_m$$

$$\frac{\Delta\beta}{\gamma} = -\frac{\tan^{-1}\left[f(t)\cos\Phi\right]}{\sin^{-1}\left[p\, f(t)/V_m\right]} \qquad (8)$$

But since the sine and tangent of small angles are approximated by the radian measure of the angles,

then

$$-\frac{\Delta\beta}{\gamma} = \frac{1}{p}\,\frac{V_m \cos\Phi}{R}$$

or

$$-\Delta\beta = \frac{1}{p}\left(\frac{V_m \cos\Phi}{R}\right)\gamma \qquad (9)$$

This shows the presence of an integrator in the geometric feedback.

The product of the transfer characteristics of all the individual elements of the constant true bearing control loop gives its open loop transfer characteristic.

$$\mu_1 = \left(\frac{p}{\omega_1}\right)\left(k_a\right)\left(\frac{R}{\cos\Phi}\right)\left(\frac{\omega_e}{p}\right)\left(\frac{\omega_3 + p}{\omega_3}\right)\left(\frac{\omega_4}{p}\right)\left(\frac{V_m \cos\Phi}{R}\right) = \frac{k_a V_m \omega_e \omega_4}{\omega_1 \omega_3}\left(\omega_3 + p\right)\left(\frac{1}{p_2}\right)$$

where

$$k_a = \mu_a/V_m$$

ω_2 can be designated as $k_a\omega_e$ and ω_5 equal to V_m/(one unit of range) since k_1 is a constant and V_m is relatively constant for the Skylark missile. The resulting open loop transfer characteristic is:

$$\mu_1 = \frac{\omega_2\ \omega_4\ \omega_5}{\omega_1\ \omega_3}\left(\frac{\omega_3 + p}{p^2}\right) \qquad (10)$$

It is obvious from Figure 6 that the effect of missile heading on the true bearing line from missile to target is exactly the same in magnitude but opposite in direction to the change of this bearing line causing the control action. Therefore, the feedback is 100 percent and negative. The closed loop transfer characteristic is:

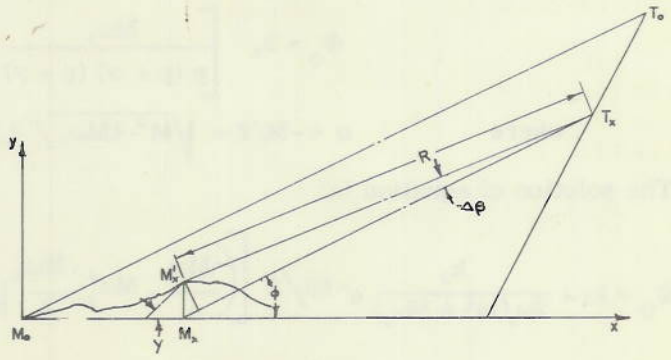

Figure 6

$$A_1 = \frac{B_o}{B_i} = \frac{\mu_1}{1 + \mu_1}$$

$$= M\left(\frac{\omega_3 + p}{p_2}\right) \Big/ 1 + M\left(\frac{\omega_3 + p}{p_2}\right)$$

$$= \frac{M\omega_3}{p^2 + M_p + M\omega_3} + \frac{Mp}{p^2 + M_p + M\omega_3} \qquad (11)$$

where $M = \omega_2\ \omega_4\ \omega_5 / \omega_1\ \omega_3$

The stability of the system may be investigated in the usual manner by obtaining the roots of the denominator of the closed loop characteristic. The roots are:

$$-M/2 \pm \sqrt{M^2 - 4\ M\omega_3}/2$$

The system is stable for all values of M, since it is impossible for the real component of either root to be positive, and for:

(1) $M > 4\omega_3$ the system is overdamped

(2) $M = 4\omega_3$ the system is critically damped

(3) $M < 4\omega_3$ the system is underdamped

One method of evaluating the values of M and ω_3 that are most applicable to the Skylark missile is to obtain the transient response of the system to a step function input for various values of these two parameters. The physical situation that would give the best means of evaluation is the one in which constant true bearing control is initiated with the missile heading in a direction that does not satisfy the control equation $\dot{\beta} = 0$. This represents a step function error in Φ, where Φ is the angular difference between the true bearing from the missile to the target and the actual heading of the missile. Since breaking the loop at the missile output results in the same closed loop servo equation as breaking the loop at the input to the missile, the transient response of the missile to a step function error in missile heading can be obtained as follows:

$$\Phi_o = \frac{M\omega_3 + M_p}{p^2 + M_p + M\omega_3} \quad \Phi_i = \frac{M\omega_3 + M_p}{p^2 + M_p + M\omega_3} \quad \frac{k_2}{p} \qquad (13)$$

where k_2/p is the Fourier transform of the step function of amplitude k_2. Breaking the equation up into the form best applicable to solution by use of Fourier transforms:

$$\Phi_o = k_2 \left[\frac{M\omega_3}{p\,(p+\alpha)\,(p+\gamma)} + \frac{M}{(p+\alpha)\,(p+\gamma)} \right]$$

where $\alpha = -M/2 + \sqrt{M^2 - 4M\omega_3}\,/\,2$; $\gamma = -M/2 - \sqrt{M^2 - 4M\omega_3}\,/\,2$

The solution of equation is:

$$\Phi_o = k_2 + \frac{k_2}{2\omega_3(M^2 - 4M\omega_3)}\, e^{-Mt/2} \left[\left(\frac{-M\omega_3}{4} + M\omega_3^2 - \frac{-M\omega_3}{4} \sqrt{M^2 - 4M\omega_3} \right) e^{-\frac{t}{2}\sqrt{M^2 - 4M\omega_3}} \right.$$

$$\left. + \left(-\frac{M\omega_3}{4} + M\omega_3^2 + \frac{M\omega_3}{4} \sqrt{M^2 - 4M\omega_3} \right) e^{\frac{t}{2}\sqrt{M^2 - 4M\omega_3}} \right] \qquad (14)$$

Plots of this solution for various values of M and ω_3 are given in Figure 7.

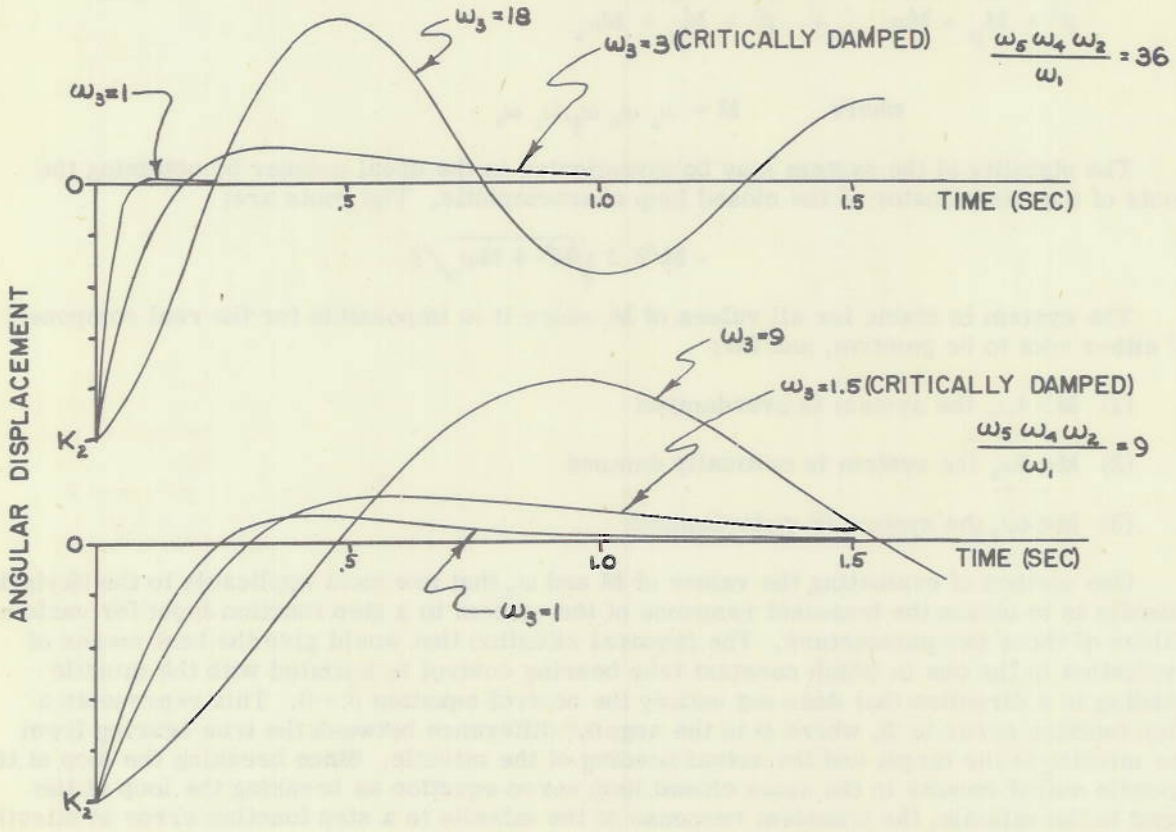

Figure 7

OWN SHIP'S ANGLE LOOP FOR SKYLARK

It has been shown in the discussion of control system requirement that it is necessary to remove missile motion from the antenna. The system to be used in Skylark is shown in Figure 8. The autopilot rate gyro will act as a differentiator over the band of frequencies

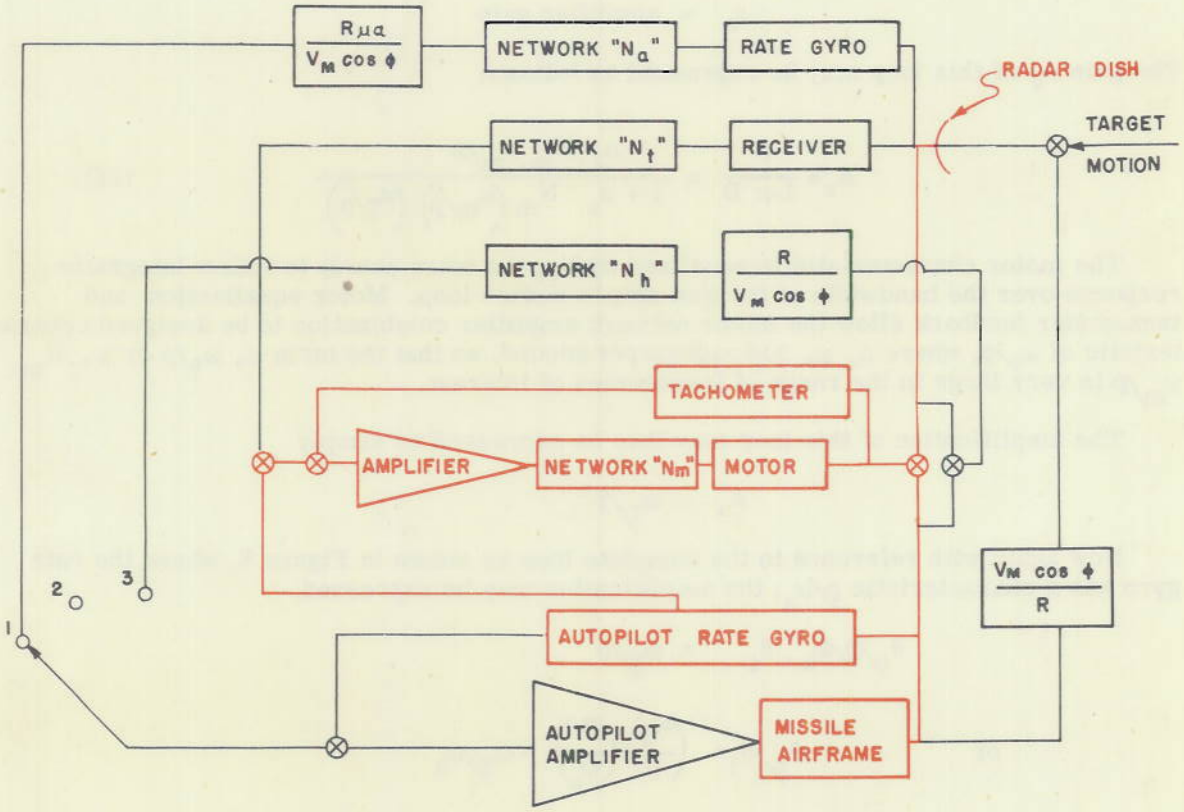

Figure 8

through which the own ship's angle loop will operate. The bandpass of the own ship's angle loop will be about 20 radians/sec., which is sufficiently in excess of the resonant frequency of the Lark airframe to provide correction at this frequency. In order to study the own ship's motion loop a study of the motor tachometer loop is first made in Figure 9

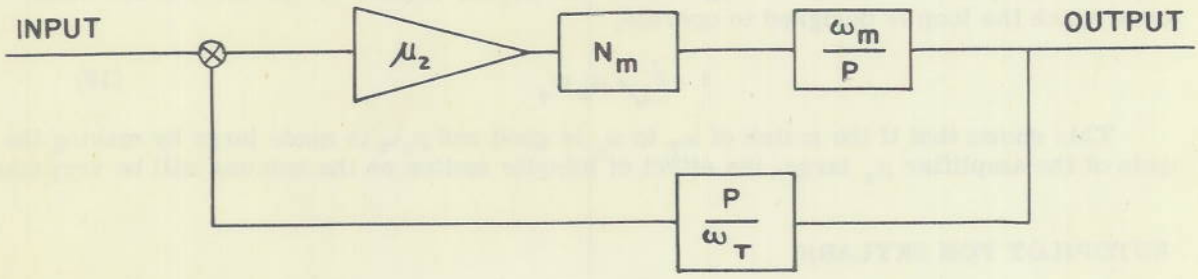

Figure 9

ω_m = motor corner,

ω_T = tachometer gain,

N_m = a network,

μ_2 = amplifier gain

The gain A_2 of this loop may be expressed as follows:

$$A_2 = \frac{\mu}{1-\mu B} = \frac{\mu_2 N_m \omega_m/p}{1 + \mu_2 N_m (\omega_m/p)(\omega_T/p)} \qquad (15)$$

The motor characteristic is equalized by N_1, the more nearly to follow integrator response over the bandwidth of the own ship's motion loop. Motor equalization and tachometer feedback allow the motor network amplifier combination to be assigned a characteristic of ω_6/p, where $\mu_2 \omega_6 >> 0$ radians per second, so that the term $\mu_2 \omega_6/p$ or $\mu_2 N_m \omega_m/p$ is very large in the range of frequencies of interest.

The amplification of this loop may then be expressed as simply

$$A_2 = \omega_T/p$$

Now again with reference to the complete loop as shown in Figure 8, where the rate gyro has a characteristic p/ω_a, the amplification may be expressed,

$$\theta_0/p/\omega_a \quad \theta_i = \omega_T/p$$

or

$$\theta_0/\theta_i = \left(\frac{\omega_T}{p}\right)\left(\frac{p}{\omega_a}\right) = \omega_T/\omega_a$$

It is apparent that all that is necessary to make the input equal the output over the range of angular frequencies for which the assumptions are valid is to make

$$\omega_T = \omega_a$$

This amounts to an adjustment of the tachometer gain level to match the gyro. Then, with the output equal to the input, the effect of missile motion on the antenna will be approximately zero. The error expression will be, for angular frequencies in the range over which the loop is designed to operate,

$$\epsilon = \dot{\theta}_i / \mu_2 \omega_6 \qquad (16)$$

This shows that if the match of ω_T to ω_a is good and $\mu_2 \omega_6$ is made large by making the gain of the amplifier μ_2 large, the effect of missile motion on the antenna will be very small.

AUTOPILOT FOR SKYLARK

One requirement of the system as assigned, is that the missile auto pilot combination act as an integrator for external or constant true bearing input signals. This autopilot will

have high gain at low frequencies of input signal and will cut off at a reasonably high frequency. It is not necessary to use this particular autopilot with this homing system, but this presents one possible solution to the autopilot problem. It may be noted that the transfer characteristic for the airframe, that is the output flight angle due to an input flap deflection has been expressed as ω_8/p. This expression is an approximation for the true transfer characteristic,

$$\frac{\Phi_o}{\delta_f} = \frac{1 + p/\omega_{15}}{p/\omega_{16}\,(1 + p/\omega_{17})\,(1 + p/\omega_{18})} \qquad (17)$$

At low frequencies of input with respect to ω_{16}, all terms except the p/ω_{16} term approach 1 and have little effect. Analysis of the effect of the terms containing ω_{15}, ω_{17}, and ω_{18} is necessary, in order to ascertain that they do not unfavorably affect stability. Further discussion appears in Appendix II.

In this analysis of the autopilot the rate gyro is assumed to have the characteristic of a differentiator over the band of frequencies of interest. To have a stable autopilot loop for Skylark the resonant frequency of the gyro must be about 200 radians per second. Further discussion of rate gyro characteristics is given in Appendix I. The effect of variation of the rate gyro characteristic from that of a pure differentiator when combined with the airframe characteristics is shown in Appendix III.

In Figure 10, the control signals are fed into the autopilot at (1). External disturbances

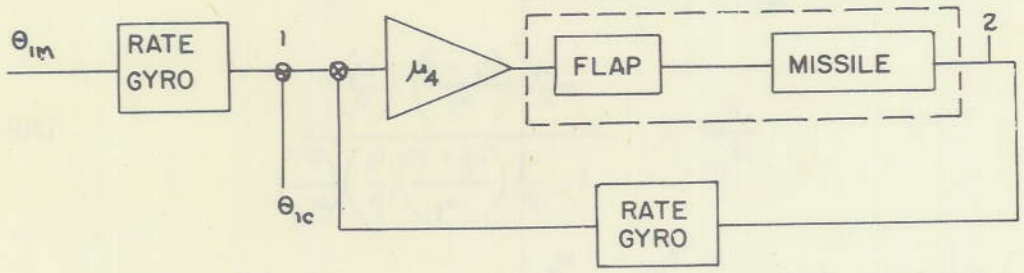

Figure 10

will cause the missile angle to change, hence are actually measured at (2). In this diagram, there are two rate gyros pictured, whereas only one is present in the actual loop. The one on the left is phantom, placed there for simplicity of explanation. The input signal fed into circuit (2) and fed back to (1) is exactly the same as if it were place in the system a $\theta_1 M$ and differentiated by the phanton rate gyro and fed into the loop at (1). The action of the autopilot to the two types of input signals, those caused by external disturbances to the missile and those signals fed into the autopilot by the control system will be investigated.

It is desired, first, to investigate the stabilizing action of the autopilot in response to external disturbances to the missile. If $\theta_{1\,M}$ is the input disturbance from the missile and θ_o is the output from the missile caused by this input, the following equations for the loop can be set up.

$$\frac{\theta_o}{\theta_{1M}\,\omega_a/p} = \frac{\mu_4\,\omega_8/p}{1 + \mu_4(\omega_8/p)\,(p/\omega_a)} \qquad (17)$$

$$\frac{\theta_o}{\theta_{1M}} = \frac{\mu_4 \left(\omega_s/p\right)\left(\omega_a/p\right)}{1 + \mu_4 \left(\omega_s/p\right)\left(p/\omega_a\right)} \tag{17}$$

From operational considerations, the gain of the control amplifier, μ_4, should have the following characteristics,

$$\mu_4 = \frac{\omega_f}{p}\left(\frac{\omega_f + p}{\omega_f}\right) \tag{18}$$

so that

$$\frac{\theta_o}{\theta_{1M}} = \frac{\omega_f/p \left(1 + p/\omega_f\right)\left(\omega_s/\omega_a\right)}{1 + \omega_f/p \left(1 + p/\omega_f\right)\left(\omega_s/\omega_a\right)} \tag{19}$$

If μ B is large $\left[\frac{\omega_f}{p}\left(\frac{\omega_f + p}{\omega_f}\right)\left(\frac{\omega_s}{\omega_a}\right) >> 1\right]$, then the error expression, for low angular frequencies of input, is,

$$\epsilon_M = \frac{\dot{\theta}_{1M}}{\frac{\omega_f\ \omega_s}{\omega_a}}$$

It is desired to study the effect of the autopilot on control signals, so a signal θ_{1c} is fed in at (1) and the output θ_{oc} at (2) is observed

$$\frac{\theta_{oc}}{\theta_{1c}} = \frac{\frac{\omega_f}{p}\left(\frac{\omega_f + p}{\omega_f}\right)\left(\frac{\omega_s}{p}\right)}{1 + \frac{\omega_f}{p}\left(\frac{\omega_f + p}{\omega_f}\right)\left(\frac{\omega_s}{p}\right)\left(\frac{p}{\omega_a}\right)} \tag{20}$$

If μ B is large, then $\frac{\theta_{oc}}{\theta_{1c}} = \frac{\omega_a}{p}$

$$\theta_{oc} = \omega_a \int \theta_{1c}$$

This shows that the missile autopilot combination is an integrator of the input control signals, which was a specification set for the operation of the design. Hence, ω_4 used elsewhere in this analysis has the value ω_a.

To obtain the desired gain of the control amplifier a circuit shown in Figure 11 is used.

The transfer characteristic of the amplifier μ_5 and motor combination will be made large, by making μ_5 large, so that the gain to the complete closed loop may be expressed.

$$\frac{E_f}{E_i} = -\frac{1}{B} = \frac{\omega_f}{p}\left(\frac{\omega_f + p}{\omega_f}\right) \tag{21}$$

where $\omega_f = \frac{1}{R_1 C_1}$

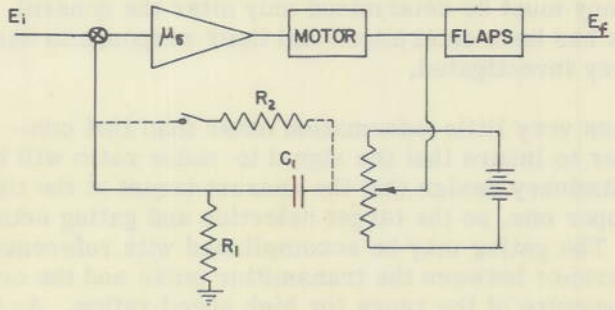

Figure 11

R_2 is a very high value resistor which will feed back to the input a very small voltage, proportional to the position of the flaps. This is to keep the flaps centered while the missile is on the ramp and during the booster period of the flight. At separation the switch is opened and the voltage is no longer fed back, hence, has no effect on the action of the autopilot during flight.

RADAR TRACKING LOOP FOR SKYLARK

In a recent conference on the Skylark program, it was decided that, due to lack of time available for development of a new type of automatic radar tracking system, a conventional passive conical scan radar assembly would be employed in the first version of the Skylark control system. The primary source of r-f power was to be a SP type radar, with the homing system utilizing a gymbaled antenna assembly with either a nutating dipole assembly or a rotating dish mounted off-center to produce the conical scan.

Skylark specifications make the use of "S" band mandatory, and missile dimensions set the size of the radar dish at a maximum of approximately nine inches. Further elaboration on the physical aspects of the tracking radar system do not come within the scope of this recommendation, as the primary concern is with the transmission system necessary to obtain the type of homing course desired.

On the basis of previous experience with tracking radars, tentative specifications on the homing receiver can be set down as follows:

(1) Tunable to SP frequency

(2) Based on a scan frequency of at least 98 cycles per second (615 radians/sec.) the side-band transmission of the separater circuits and system, before equalization, should be flat to 25 cycles per second (157 radians/sec).

(3) Maximum detectable signal to minimum detectable signal ratio at least $\frac{1000}{1}$

(4) Maximum sensitivity

(5) Slope at gain crossover less than -45^{o}

(6) The scan frequency of the antenna must be set in a region where the twenty-four cycle scan frequency of the SP and the tracking sidebands or harmonics of both cannot materially affect the tracking of the homing system. This will almost certainly mean that the scan frequency of the automatic tracking system must be high. The

selection of the actual scan frequency must be determined only after the general circuitry of demodulation networks has been determined and their response to harmonics of the homing scan frequency investigated.

The receiver must be gated so as to pass very little information other than that contained in the echoes from the target, in order to insure that the signal to noise ratio will be acceptable. It can be assumed for this preliminary design that the nearest target at the time of the initiation of homing control is the proper one, so the target selection and gating action can be controlled inside the missile itself. The gating may be accomplished with reference to the transmitter pulse, with the time-difference between the transmitter pulse and the echo from the target being a good approximate measure of the range for high speed ratios. As the gain of the constant true bearing control system is to be inversely proportional to the range between the missile and the target, it is necessary that some range measurement be made. This measurement is accomplished when the range gate follows the target. Conventional multivibrators and conventional sweep circuits may be used to provide not only the range following characteristic but, in addition, may be employed to give a range sweep that will allow searching for the target before the start of homing.

It is possible that the transmitter pulse used for reference may be picked off the output of the homing receiver, but it is probably advisable to use the output of the mid-course receiver to provide this reference because of possible propagation difficulties and possible homing receiver blocking. Gating of the homing receiver so as to make it sensitive only during the relatively short time which would insure proper range tracking would eliminate possible blocking. Pulse stretching techniques should be employed in the design to increase the signal to noise ratio to a maximum.

The general features of the low frequency portion of the automatic tracking loop can be set up in several ways in accordance with the usual servo-loops for conventional automatic tracking systems.

Assuming the action of the own ship's angle loop is such that it is capable of transmitting both own ship's angle + radar tracking signals to a higher degree of accuracy than the radar tracking system can follow (i. e. the error of the own ship's angle loop has errors containing only high frequency components), there is no internal coupling between the two loops, and therefore there is no effect on true antenna heading by changes in missile heading, except that reflected through the target. Under this assumption, the radar tracking loop can be set up as shown in Figure 12.

The characteristics of elements in the block diagram are as follows:

(1) The output of the receiver is to indicate linearly errors in antenna tracking for small angles and low frequencies. We can merely ascribe to it a gain constant k_r whose units are volts per radian.

(2) The characteristics of N_t will be investigated in the following pages. It is merely an equalizing network-amplifier combination, whose design will determine the error characteristic of this loop.

(3) The amplifier, motor, and tachometer combination are units of the own ship's angle system. This portion of that loop has a transfer characteristic of ω_a/p over a much higher range of frequencies than needed for the response of the radar tracking loop. ω_a specifies the operating level of this portion of the circuit.

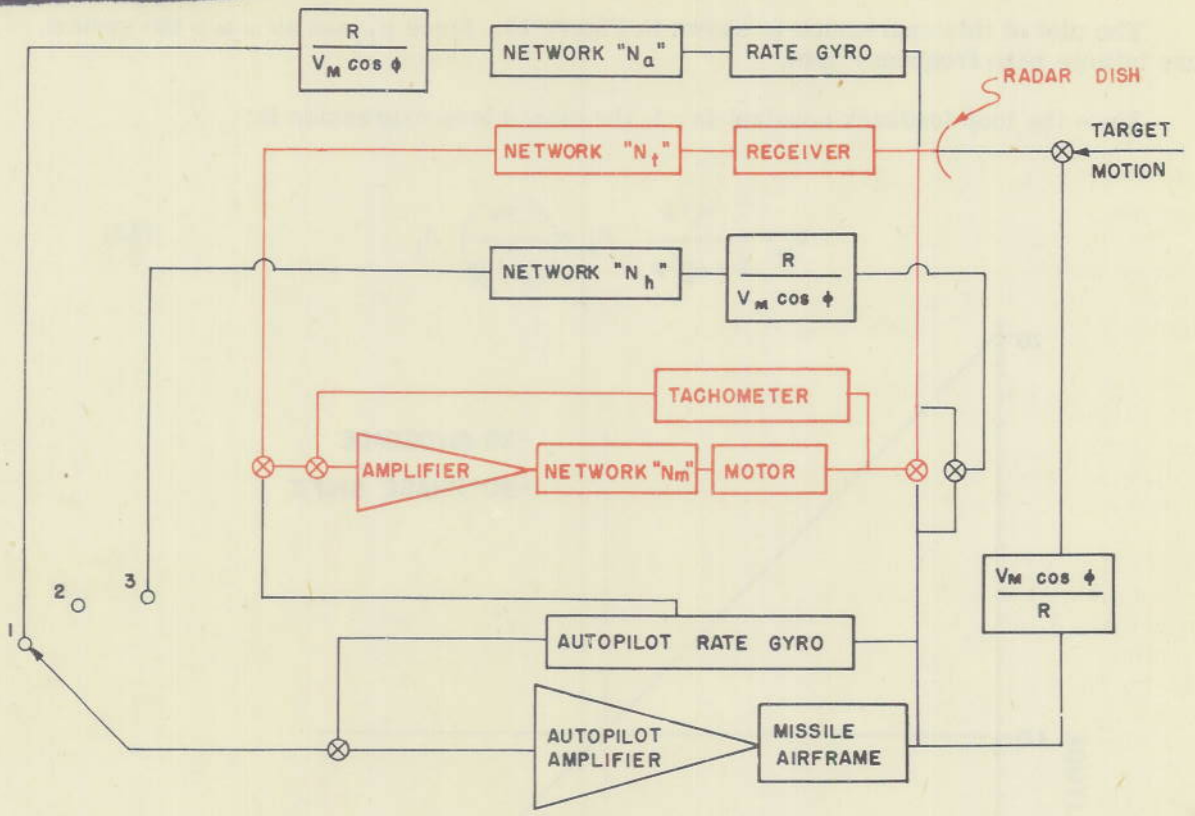

Figure 12

The specifications of N_t can best be made on the basis of the error characteristic we desire our automatic tracking loop to have. We shall investigate three possible error characteristics. These are:

(1) $\epsilon \alpha$ to the rate of change of the antenna line of sight angle

(2) $\epsilon \alpha$ to the acceleration of the antenna line of sight angle

(3) $\epsilon \alpha$ to a combination of (1) and (2).

These error characteristics are for low angular frequencies of input and are the usual servo error characteristics.

To obtain the error characteristic listed first, all that is necessary is to set N_t equal N_{t1}, a linear amplifier or a straight through feed if the receiver video operating level can be varied. For purposes of analysis, the gain constant associated with N_t (or video operating level, if that can be varied) as k_b will be carried.

The open loop transfer characteristic, considering the loop broken at the antenna, can then be written:

$$\mu_{t1} = (\text{Receiver Angular Sensitivity}) \left(k_b\right) \left(\omega_y/p\right) = \omega_g/p \qquad (22)$$

The plot of this expression is shown in Figure 13. Since $\mu_{t_1} \to \infty$ as $\omega \to 0$ the system has infinite zero frequency gain.

Since the loop feedback constant is -1, the closed loop expression is:

$$\beta_o = \frac{\omega_g/p}{1 + \omega_g/p} \quad \beta_i = \left(\frac{\omega_g}{\omega_g/+ p}\right) \beta_i \tag{23}$$

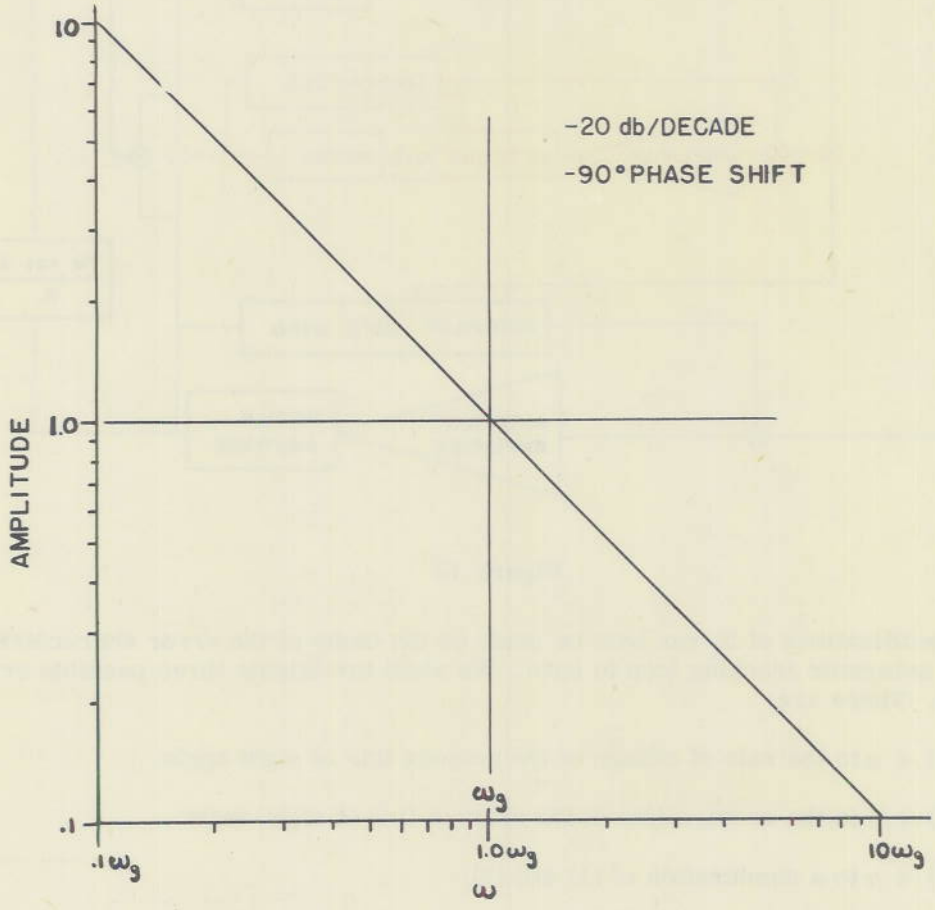

Figure 13

This is plotted in Figure 14. The bandpass of the system is evidently ω_g, and the error characteristic is,

$$\epsilon_{t_1} = \frac{\beta_i}{1 + \omega_g/p}$$

and for low angular frequencies $(\omega_g/p \gg 1)$

$$\epsilon_{t_1} = \dot{\beta}/\omega_g \tag{24}$$

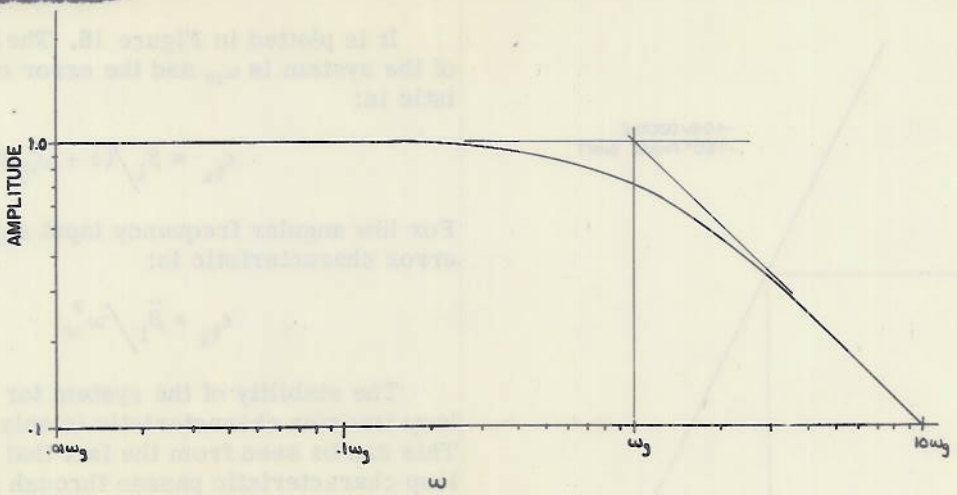

Figure 14

The fact that the system is stable and critically damped is evident from the fact that it has -45^0 phase shift at gain crossover.

Stability can also be shown in the classical manner by obtaining the response of the system to a step function input in the following manner.

$$\beta_o = \frac{\omega_g \beta_i}{p + \omega_g} \quad 1, \quad \beta_o = \frac{\omega_g}{p\,(p + \omega_g)} \tag{25}$$

The root of the demoninator of the expression for "A" is obviously real and negative showing the system is at least critically damped. The solution is,

$$\beta_o = 1 - e^{-\omega_g t} \tag{26}$$

for a step function input of amplitude unity. This shows the system to be critically damped.

A simple transfer characteristic to make error proportional to acceleration can be obtained by setting the network N_t equal N_{t_2} a pure integrator, i.e.,

$$N_{t_2} = \omega_n / p \tag{27}$$

Where ω_n specifies the operating level of the network, ω_n is that angular frequency of pure sine wave input that gives an output whose amplitude is equal to the input amplitude.

The open loop transfer characteristic of the radar tracking loop will then be μ_{t_2} = (Receiver angular sensitivity) $(\omega_n/p)\ (\omega_g)/p = \omega_{10}^2/p^2$, which is plotted in Figure 15.

The closed loop expression is:

$$\frac{\beta_o}{\beta_i} = \omega_{10}^2/p^2 + \omega_{10}^2 \tag{28}$$

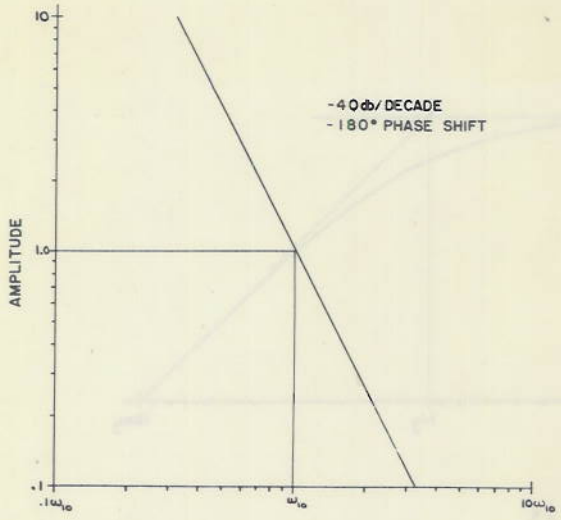

Figure 15

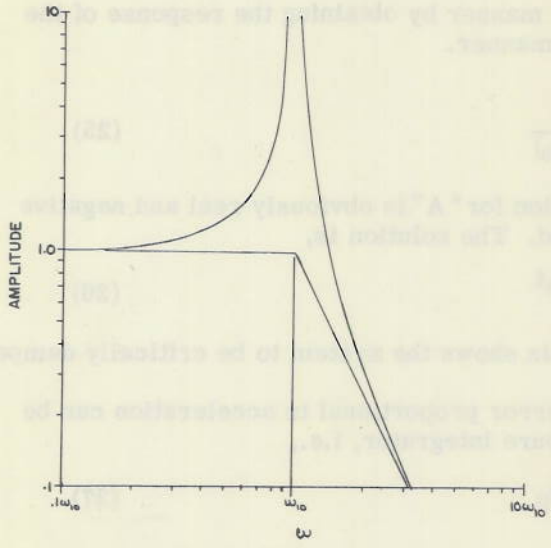

Figure 16

It is plotted in Figure 16. The bandwidth of the system is ω_{10} and the error characteristic is:

$$\epsilon_{t_2} = \beta_i \Big/ (1 + \omega_{10}^2/p^2)$$

For low angular frequency input signals the error characteristic is:

$$\epsilon_{t_2} = \ddot{\beta}_i \Big/ \omega_{10}^2 \qquad (29)$$

The stability of the system for the open loop transfer characteristic is only marginal. This can be seen from the fact that the open loop characteristic passes through gain crossover with a phase shift of -180^0 and consequently the phase shift of the closed loop transfer characteristic changes from 0 to -180^0 at gain crossover. This means that the system oscillates. Illustrating by solution of the differential equation of motion of the system for a unit step function input:

$$\beta_o = \frac{\omega_{10}^2}{p^2 + \omega_{10}^2} \qquad (1)$$

$$\text{or} \quad \frac{d^2 \beta_o}{dt^2} + \omega_{10}^2 \beta_o = \omega_{10}^2 \quad 1 \qquad (30)$$

which has a general solution

$$\beta_o = 1 - \cos \omega_{10} t \qquad (31)$$

Obviously, such a system is unusable as it stands, but by equalization at gain crossover, the system can be made stable without materially affecting the error characteristic or bandpass of the system. If, as in the usual case, a system is designed which is slightly underdamped, it is only necessary to insert a simple network having the transfer characteristic,

$$\mu_{eq} = \frac{\omega_{10} + p}{\omega_{10}} \qquad (32)$$

A plot of this characteristic is shown in Figure 17. This modifies the transmission characteristic to,

$$\mu'_{t_2} = \frac{\omega_{10}^2}{p^2} \left(\frac{\omega_{10} + p}{\omega_{10}} \right) \qquad (33)$$

Which plots are shown in Figure 18.

The closed loop transfer characteristic A_2 is then:

$$\beta_o = \frac{\frac{\omega_{10}^2}{p^2}\left(\frac{\omega_{10}+p}{\omega_{10}}\right)}{1+\frac{\omega_{10}^2}{p^2}\left(\frac{\omega_{10}+p}{\omega_{10}}\right)}\beta_i \qquad (34)$$

The phase shift at gain crossover for the closed loop is half that of the open loop at that point and is equal to $-67\frac{1}{2}^0$. This means the system is stable and is slightly under critically damped. The degree of damping can be adjusted if desired by adjusting the crossover frequency of the equalizing network, inserted to make the system stable, to be either higher or lower than corner frequency of the unequalized system. If the corner of the equalizer is lower than the unequalized corner frequency, the degree of damping will be increased, if higher the degree of damping will be decreased. This can be shown in the conventional manner as follows:

$$\beta_o = \frac{\omega_{10}^2 + \omega_{10}p}{p^2 + \omega_{10}p + \omega_{10}^2}\beta_i \qquad (35)$$

For a unit step function input,

$$\beta_o = \frac{\omega_{10}^2 + \omega_{10}p}{p(p+\alpha)(p+\gamma)}$$

where $\alpha = -\frac{\omega_{10}}{2} + i\frac{\sqrt{3}}{2}\omega_{10}$

$$\gamma = -\frac{\omega_{10}}{2} - i\frac{\sqrt{3}}{2}\omega_{10}$$

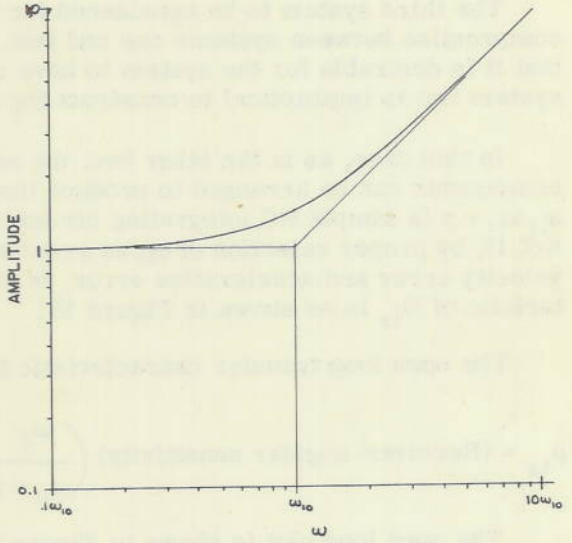

Figure 17

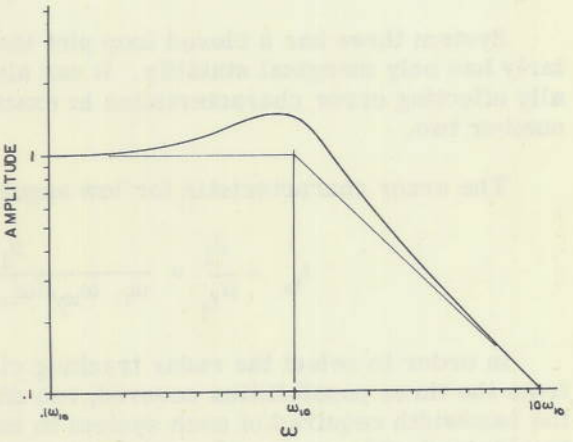

Figure 18

Since the roots of the denominator contain only negative real components and imaginaries, the system is stable. The solution of equation (35) is:

$$\beta_o = 1 - \omega_{10}\, e^{-\omega_{10}t/2}\left[\frac{1}{\sqrt{3}}\sin\left(\frac{\sqrt{3}}{2}\omega_{10}t\right) + \cos\left(\frac{\sqrt{3}}{2}\omega_{10}t\right)\right] \qquad (36)$$

This solution indicates that the statements made on the basis of the phase shift at gain crossover are true and the conclusions are valid.

The third system to be considered for the radar tracking loop is one which is really a compromise between systems one and two. This compromise may be necessary if it is found that it is desirable for the system to have characteristics similar to system number two, and system two is impractical to construct for this application.

In this case, as in the other two, the network N_t can be the point in the circuit where components can be arranged to produce the desired error characteristic. By setting $N_{t_3} = \omega_{11}/\omega_{11} + p$ (a simple RC integrating circuit where ω_{11} is less than the bandwidth of system No. 1), by proper selection of ω_{11} an error expression with the desired balance between velocity error and acceleration error, is obtained. A typical plot of the transfer characteristic of N_{t_3} is as shown in Figure 19.

The open loop transfer characteristic for system No. 3 is then,

$$\mu_{t_3} = (\text{Receiver angular sensitivity}) \left(\frac{\omega_{11}}{\omega_{11} + p}\right) \left(\frac{\omega_y}{p}\right) = \frac{\omega_{11}\omega_{12}}{(\omega_{11} + p)\, p} \qquad (37)$$

The open loop plot is shown in Figure 20, where $\omega_{12} = \omega_y$ (receiver angular sensitivity). The closed loop plot is shown in Figure 21. The bandpass is

$$\sqrt{\omega_{11}\omega_{12}}$$

System three has a closed loop plot identical to that for system number two, and similarly has only marginal stability. It can also be stabilized to make it stable without materially affecting error characteristics in exactly the same way that was given for system number two.

The error characteristic for low angular frequencies of input for this possibility is:

$$\epsilon_{t_3} = \frac{\beta_i}{\mu_{t_3}} = \frac{\beta_i}{\omega_{11}\,\omega_{12}/(\omega_{11} + p)\, p} = \frac{\ddot{\beta}}{\omega_{11}\,\omega_{12}} + \frac{\dot{\beta}}{\omega_{12}} \qquad (38)$$

In order to select the radar tracking circuit that is best for this particular application from the three possibilities covered, two different properties must be considered. First, the bandwidth required of each system to have identical magnitudes of following error must be obtained. The system requiring the least bandwidth to track to the degree of accuracy required without considering the effect of noise will have the best characteristics when subjected to noise. Second, the effect of lapses in the flow of control information must be investigated for each system. The system which keeps in motion most nearly at a constant rate will have the least probability of losing the target during such a period, and in addition keeps the information derived from the radar system from having violent discontinuities due to momentary lapses in information from the target.

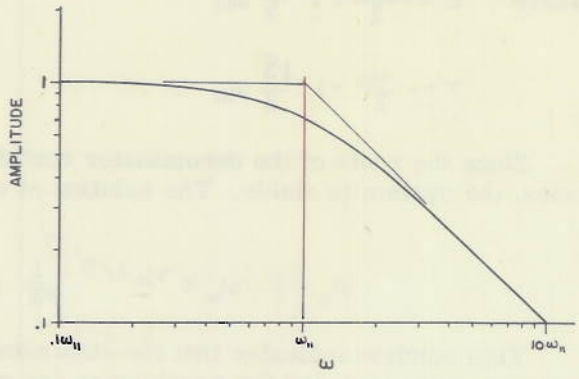

Figure 19

The error characteristics for the three systems are:

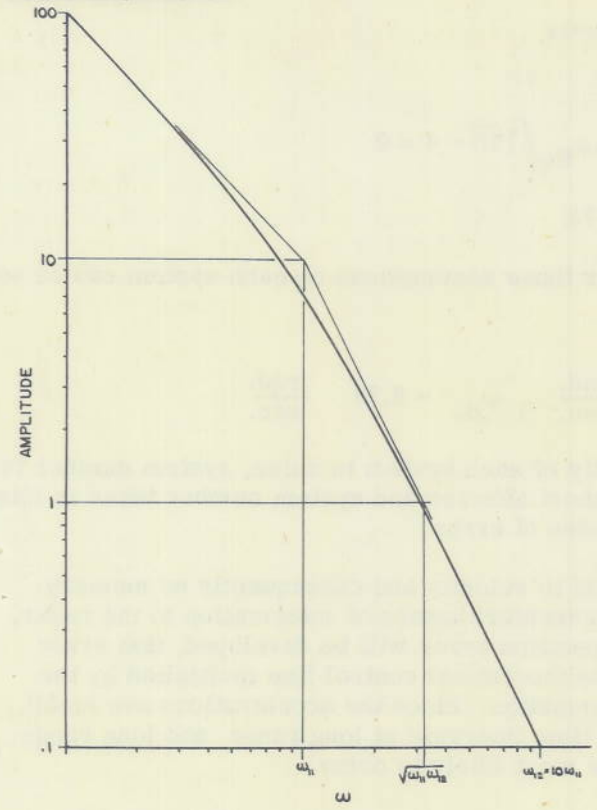

Figure 20

$$\epsilon_{t_2} = \epsilon_{t_1} \quad ; \quad \dot{\beta}/\omega_9 = \ddot{\beta}/\omega_{10}^2$$

Then if ω_9 is greater than one radian per second, the bandwidth required for system number two is less than that required by system one for the same accuracy. Under the assumption that the bandwidth requirement of system number one is approximately 4 radians per second, then

$$\omega_{10} = 2 = \omega_9/2$$

To compare the bandwidth requirements for systems one and three under the same assumptions:

$$\epsilon_{t_1} = \epsilon_{t_3} \quad ; \quad \dot{\beta}_i/\omega_9 = \ddot{\beta}_i/\omega_{11}\omega_{12} + \dot{\beta}_i/\omega_{12}$$

but $\omega_{11} = \omega_{12}/\sqrt{10}$, and therefore

$$\frac{1}{\omega_9} = \frac{1}{\omega_{B3}^2} + \frac{1}{\sqrt{10}\,\omega_{B3}}$$

$$\epsilon_{t_1} = \dot{\beta}/\omega_9$$

$$\epsilon_{t_2} = \ddot{\beta}/\omega_{10}^2$$

$$\epsilon_{t_3} = \ddot{\beta}/\omega_{11}\omega_{12} + \dot{\beta}/\omega_{12}$$

In order to explore the relative potentialities of these systems, consider an assumption at this point to give us a basis of comparison of the different error characteristics. That assumption is: The accelerations experienced in tracking a real target are of lower magnitudes than the velocities occuring in tracking the same target, though usually out of phase with the velocities.

If we set the magnitudes of the errors of the three systems equal and set the magnitudes of the velocities equal to the magnitudes of the accelerations for a particular course, we have a basis of bandwidth comparison that favors the system having errors proportional to velocity, i.e.:

$$\epsilon_{t_1} = \epsilon_{t_2} = \epsilon_{t_3} \quad \text{and} \quad \ddot{\beta}_i = \dot{\beta}_i$$

then for systems one and two:

or $\omega_9 = \omega_{10}^2$

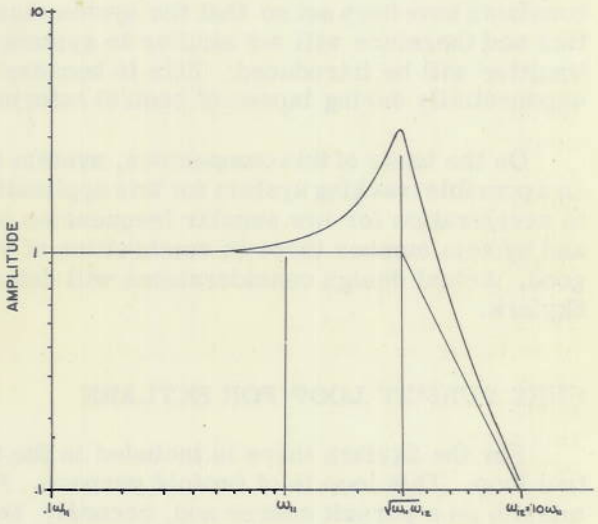

Figure 21

where $\omega_{B_3}^2 = \omega_{11}\omega_{12}$

or on the assumption that $\omega_9 = 4$

$$\omega_{B_3}^2 - 4\,\omega_{B_3}/\sqrt{10} - 4 = 0$$

which has a positive real root $\omega_{B_3} = 2.73$

Therefore the bandwidth requirements for those assumptions on each system can be set down as follows:

$$\omega_{B_1} = 4\ \frac{\text{rad.}}{\text{sec.}}\ ;\ \omega_{B_2} = 2\ \frac{\text{rad.}}{\text{sec.}}\ ;\ \omega_{B_3} = 2.73\ \frac{\text{rad.}}{\text{sec.}}$$

From the point of view of the susceptibility of each system to noise, system number two is the least affected, system number one the most affected and system number three is intermediate for systems having the same magnitudes of error.

System number one has error proportional to velocity and consequently no memory characteristics concerning velocity. During momentary lapses of information to the radar, the control line will stay fixed and a definite position error will be developed, that error being equal to the angular rate of change of the theoretical control line multiplied by the time interval of the interruption of control information. Since the accelerations are small, the velocity is relatively constant over small time intervals at long range and long range is where the lapses in control information are most likely to occur.

System two, which has error proportional to acceleration, will keep the control line moving at the rate that the control line had when control lapsed during lapses in control information. As the velocity is almost constant over short time intervals, when the control line is reestablished relatively small discontinuities will be introduced.

System three has error porportional to both velocity and acceleration, but the circuit constants have been set so that the system has relatively long velocity memory characteristics and therefore will act similar to system number two, except that slightly larger discontinuities will be introduced. This is because the velocity of the control line will decay exponentially during lapses of control information.

On the basis of this comparison, system number one is eliminated from consideration as a possible tracking system for this application, with system number two (error proportional to acceleration for low angular frequencies of input) being the best of the systems considered, and system number three (a combination of velocity and acceleration error) being almost as good. Actual design considerations will determine which will be the most applicable for Skylark.

PURE PURSUIT LOOP FOR SKYLARK

For the Skylark there is included in the terminal guidance system a pure pursuit control loop. This loop is of twofold purpose. First, for the early tests, it is desired to fly the missile on a pursuit course and, secondly, this loop may be utilized to reduce the dispersion due to launching excursions. The input to this loop will be the measured difference between the angle of the radar dish and the end heading of the missile. In order to develop a pure pursuit course this angle must be maintained at zero.

In this system the radar dish is isolated by the own ship's motion loop so that the angular motion of the missile will not affect the angle of the dish, provided the missile is roll stabilized. Therefore, if the missile changes heading during launching, this angle will not be reflected into the dish and an angle will be developed between the dish and the missile equal to the angle through which the missile has rotated. As soon as separation is complete and control established, there will be a signal fed into the autopilot proportional to this angle, which will force the missile to turn back through whatever angle it has turned. If, during the launching, the missile radar has picked up the target, then the antenna will align itself with the target and the missile will then be forced to align itself with the target, instead of heading in a direction parallel to the original launching direction. If the target is not picked up, as will usually be the case, there will be no radar error signals to alter the angle of the dish. This will cause it to remain on the same heading as it was during firing.

Hence, it may be seen from Figure 22 that the lateral dispersion is limited to that which is built up during the no control period of launching.

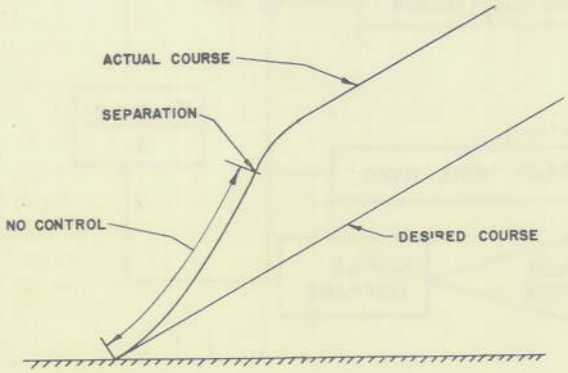

Figure 22

To obtain a pure pursuit course the angle between the radar dish and the missile will be measured and the missile autopilot will be caused to drive this angle to zero. The diagram of the loop is shown in Figure 23. This appears to be quite complex, but lends itself to considerable simplification. By separating the own ship's motion loop from the radar tracking loop as is done in Figure 24, it is possible to eliminate the action of the own ship's motion loop from this study.

It has been shown in the analysis of the own ship's motion loop that the output ψ can be made equal to zero with only very small errors. Hence, if it is assumed that it is zero, the diagram can be further simplified to take the form shown in Figure 25.

N_h, the homing correction network, is given a value $\omega_{13} + p/\omega_{13}$, a form which may be obtained with a simple R-C circuit. The equations for the various loops may now be set up.

The open loop gain in loop I, that is, the effect of the measured error signal on the angle of the missile, is as follows:

$$\frac{\theta_1}{\theta_i - \theta_3} = \frac{\omega_4}{p} \frac{\omega_{13} + p}{\omega_{13}} \tag{39}$$

The value of θ_3, the angle of the radar dish in space for an input θ_i due to target motion is, when utilizing the third radar tracking loop discussed in the previous section, as follows:

$$\frac{\theta_3}{\theta_1} = \frac{\frac{\omega_a}{p}\left(\frac{\omega_{11}}{\omega_{11}+p}\right)\left(\frac{\omega_{14}+p}{\omega_{14}}\right)k_r}{1 + \frac{\omega_a}{p}\left(\frac{\omega_{11}}{\omega_{11}+p}\right)\left(\frac{\omega_{14}+p}{\omega_{14}}\right)k_r} \tag{40}$$

where $\omega_{14} = \sqrt{\omega_{11}\,\omega_{12}} = \sqrt{10}\,\omega_{11}$ and k_r = Receiver angular sensitivity

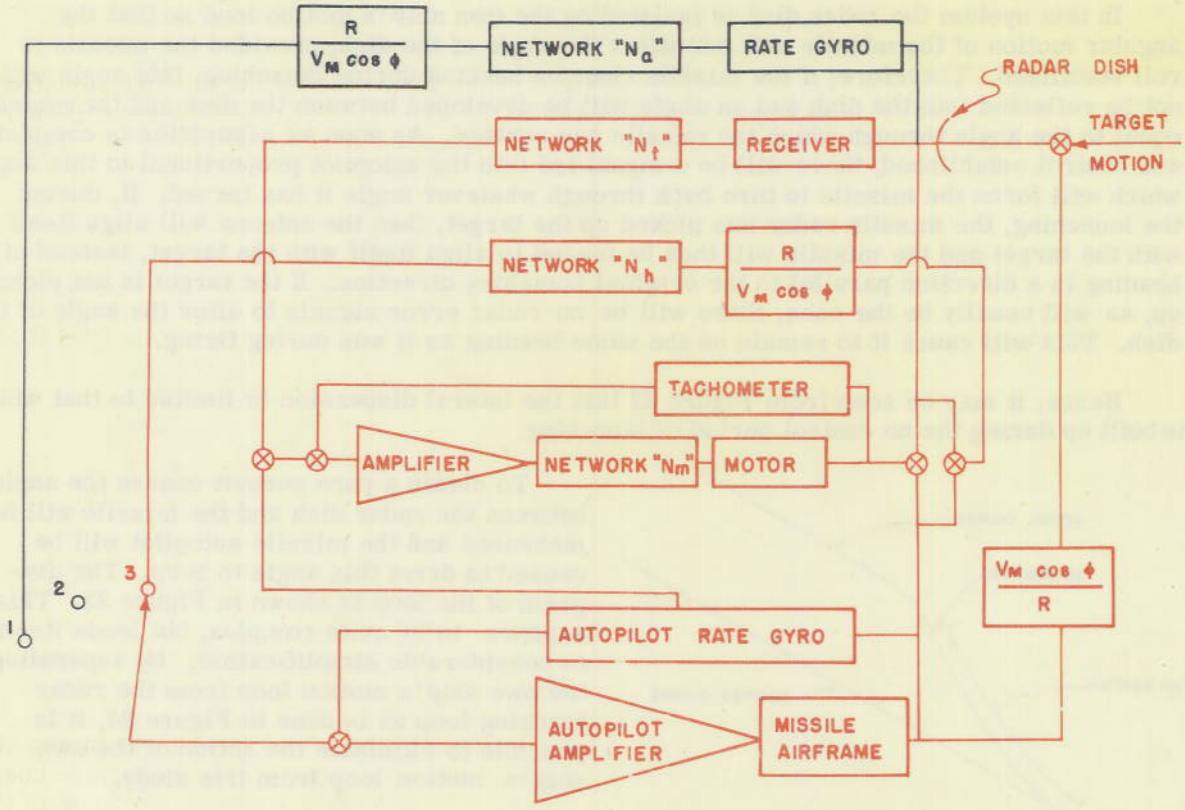

Figure 23

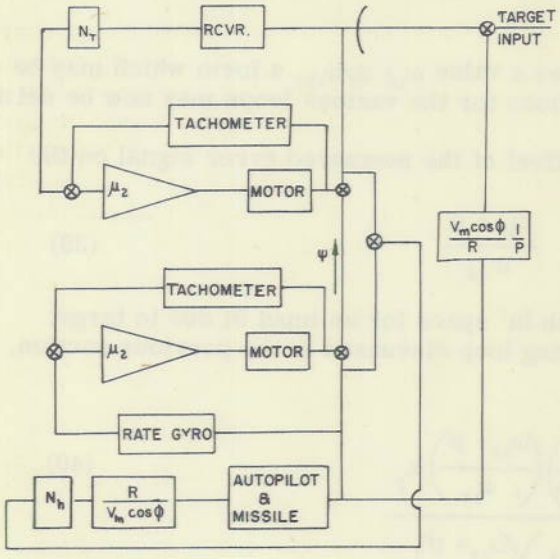

Figure 24

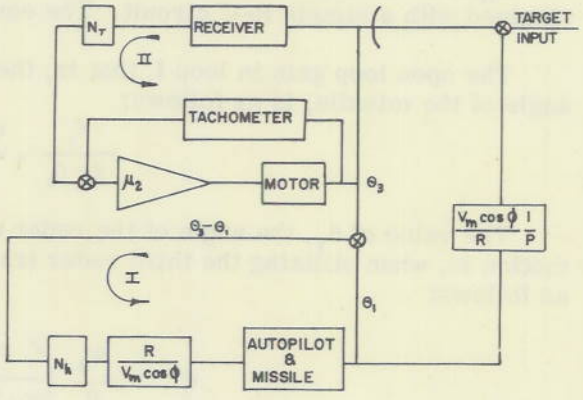

Figure 25

It is to be remembered that the amplifier-motor-tachometer combination was adjusted so that it had the transfer characteristic ω_a/p. This was necessary for the successful operation of the own ship's motion loop. The affect of the missile motion on θ_o is,

$$\frac{\theta_o}{\theta_i} = \frac{\omega_5}{p} \tag{41}$$

Combining equation 39, 40, and 41, the following open loop transfer characteristic from θ_i to θ_o is obtained

$$\mu_h = \frac{\omega_5 \quad k_r \quad \frac{\omega_a}{p} \quad \frac{\omega_{11}}{\omega_{11}+p} \quad \frac{\omega_{14}+p}{\omega_{14}} \quad \frac{\omega_4}{p} \quad \frac{\omega_{13}+p}{\omega_{13}}}{p\left[1 + k_r \frac{\omega_a}{p}\left(\frac{\omega_{11}}{\omega_{11}+p}\right)\left(\frac{\omega_{14}+p}{\omega_{14}}\right)\right]\left[\left(\frac{\omega_4}{p}\right)\left(\frac{\omega_{13}+p}{\omega_{13}}\right) - 1\right]} \tag{42}$$

If at this point the representative values discussed in the previous section are substituted for the various parameters of this equation, a plot as shown in Figure 26, is obtained.

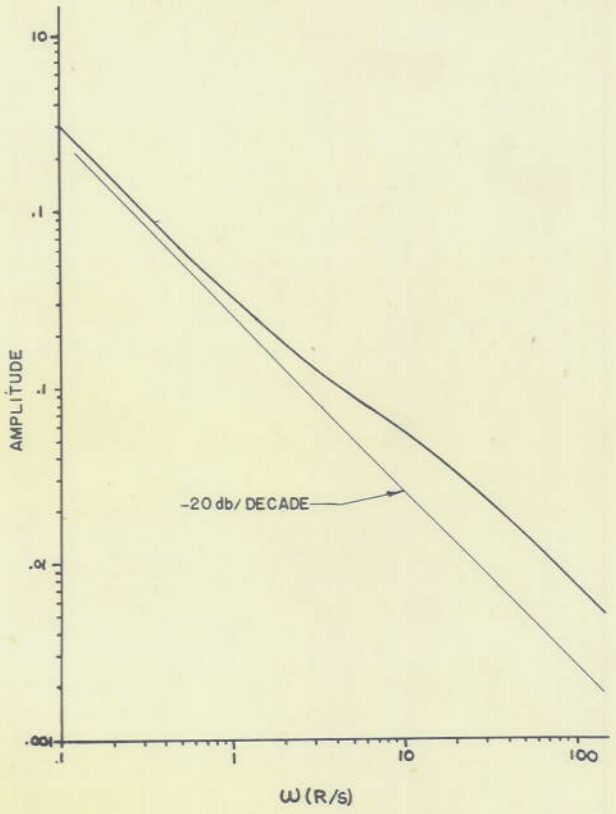

Figure 26

Small changes in the values of any of the parameters of this equation have been seen to have little affect on the form of the curve, but will change the gain and bandwidth of the system. The use of another type of radar tracking loop has little effect.

This plot has a slope which approximates the -20 db per decade, characteristic of a pure integrator. Hence, it may be shown that the loop operates in a fashion similar to a loop containing an integrator and a direct feedback (B = -1). It is stable and approximately critically damped.

APPENDIX I

Rate Gyro Characteristics

Inasmuch as rate gyros perform essential functions in the constant true bearing system, it is important to know their frequency response characteristics and the bandwidth limits over which their response will make them a true following device proportional to the rate of change of input signal. It is the purpose of this appendix to exhibit these frequency response characteristics in such a fashion as to enable the proper selection of rate gyros for the purposes designed.

The purpose of a rate gyro is to give a signal output proportional to the velocity of rotation of the gyro about the gyro input axis. This is equivalent to stating that, over the performance bandwidth required of a particular gyro, it has an amplitude of output versus frequency plot showing a linear 20 db per decade rise on log-log paper with a constant phase shift of plus 90 degrees for a constant amplitude variable frequency input to the gyro input axis.

Start with the complete equation of the performance of a rate gyro,

$$I_g \frac{d^2\theta_g}{dt^2} + C_g \frac{d\theta_g}{dt} + K_g\theta = H\omega_i \cos\theta_g - H\omega_s \sin\theta_g - I_g \frac{d\omega_o}{dt} + M_c + M_i + M_u \qquad (1)$$

where

θ_g = gimbal angular displacement about gimbal (output) axis, with respect to the gyro case

I_g = moment of inertia of the gimbal assembly about the gimbal axis

C_g = Viscous damping coefficient
K_g = spring constant
} Gimbal with respect to case

ω = angular velocity of gyro case

ω_i = about input axis

ω_s = about secondary input axis

ω_o = about output axis

$H = I_{sp}\Omega$ = angular momentum of rotor

I_{sp} = moment of inertia of rotor

Ω = angular velocity of rotor

M_c = correction torque applied to output (gimbal) shaft (as from unbalanced weights).

M_i = torque on output shaft due to the indicating system

M_u = torque on output shaft due to uncertainties (nonviscous, coulomb, etc.).

Equation (1) considers that the gimbal is suspended so that there is but one degree of freedom of the gimbal with respect to the case, i.e., about the gimbal axis.

The following simplifications are made:

A. Let $\cos\theta_g = 1$

This is valid since θ_g maximum for a practical rate gyro is of the order of 2^0 and $\cos\theta_g$ is = 0.9994

B. $\omega_s = \omega_o$ $\theta_i = \theta_{im} \sin\omega_f t$.

That is, consider a sinusoidal motion of displacement amplitude about the input axis only. These conditions may be fulfilled exactly in a test. Under service conditions, the term in equation (1) involving ω_s is small since $\sin\theta_g$ is small, and the motion ω_o is unimportant.

C. $M_c = M_i = M_u = 0$

It is anticipated that no M_c will be applied to the simple rate gyros to be used in this application. M_i is due only to the small induction coil pickoff drag and may be neglected. M_u is small and will be neglected here.

With these modifications, the gyro equation becomes:

$$\frac{d^2\theta_g}{dt^2} + \frac{C_g}{I_g}\frac{d\theta_g}{dt} + \frac{k_g}{I_g}\theta_g = \frac{H}{I_g}\omega_i \qquad (2)$$

The undamped resonant frequency of the gyro can easily be arrived at from the general solution of the left hand side of equation (2) with the viscous damping coefficient, C_g, set equal to zero, i.e.,

$$\frac{d^2\theta_g}{dt^2} + \frac{k_g}{I_g} = 0 \qquad (3)$$

Equation (3) has a general solution

$$\theta_g = A_e^{i\sqrt{\frac{k_g}{I_g}}(t+\delta)} \qquad (4)$$

where δ is a constant determined by initial conditions.

The undamped resonant frequency of the gyro is therefore:

$$\omega_n = \sqrt{\frac{k_g}{I_g}} \qquad (5)$$

The coefficient of $d\theta_g/dt$ which makes the gyro a critically damped system can be obtained from the left-hand side of equation (2) by letting the viscous damping coefficient, C_g, be a variable as follows:

$$\frac{d^2\theta_g}{dt^2} + \frac{C_g}{I_g}\frac{d\theta_g}{dt} + \frac{K_g}{I_g}\theta_g = 0 \qquad (6)$$

or, in operational form:

$$\left\{\left[p + \left(\frac{C_g}{2I_g} + \sqrt{\frac{C_{g^2}}{4I_{g^2}} - \frac{K_g}{I_g}}\right)\right]\left[p + \left(\frac{C_g}{2I_g} - \sqrt{\frac{C_{g^2}}{4I_{g^2}} - \frac{K_g}{I_g}}\right)\right]\right\}\theta_g = 0 \qquad (7)$$

From equation (7), it can be seen that if, $C_g = 2\sqrt{k_g I_g}$ (8)

the gyro is critically damped. The damping ratio ξ is then:

$$\xi = \frac{C_g}{2\sqrt{k_g I_g}} \qquad (9)$$

where C_g/I_g is actual damping and $2\sqrt{k_g I_g}$ is critical damping.

Substituting (5) and (9) into equation (2) and expressing the resultant in operational form:

$$(p^2 + 2p\xi\omega_n + \omega_n^2)\,\theta_g = \frac{H}{I_g}\,p\,\theta_i \qquad (10)$$

or the transfer characteristic of a rate gyro under assumptions A, B, and C, is

$$\frac{\theta_g}{\theta_i} = \frac{p\frac{H}{I_g}}{p^2 + 2p\,\xi\,\omega_n + \omega_n^2} \qquad (11)$$

Plots of both the magnitude of this transfer characteristic as a function of frequency and phase shift as a function of frequency are given in Figures 27 and 28 for steady state conditions.

The actual output voltage from the rate gyro is related to θ_g by a constant. This constant is determined by the pickoff system. Its actual magnitude is unimportant so long as the pickoff assembly has sufficient sensitivity to allow the gyro to have a good signal to noise ratio, and the inductance and inertial characteristics do not alter the characteristics of the gyro itself in the range of frequencies over which the gyro is to operate.

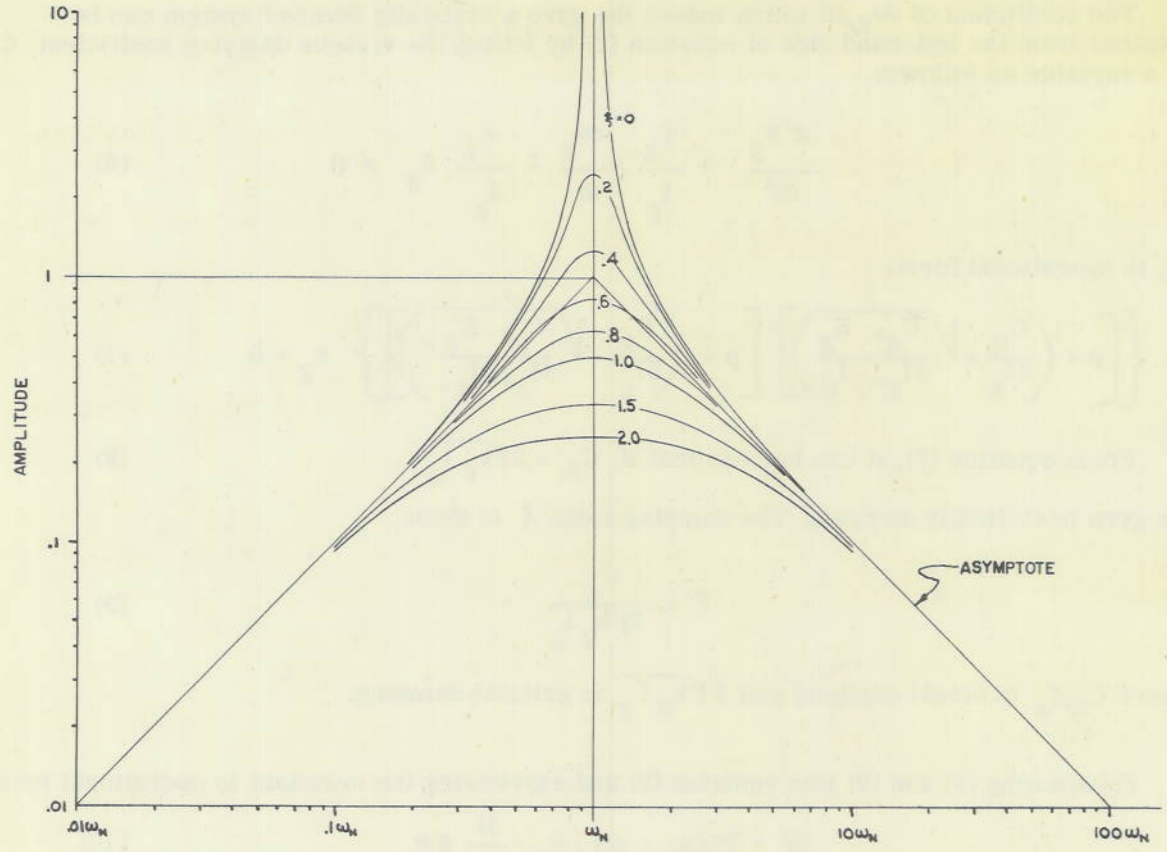

Figure 27

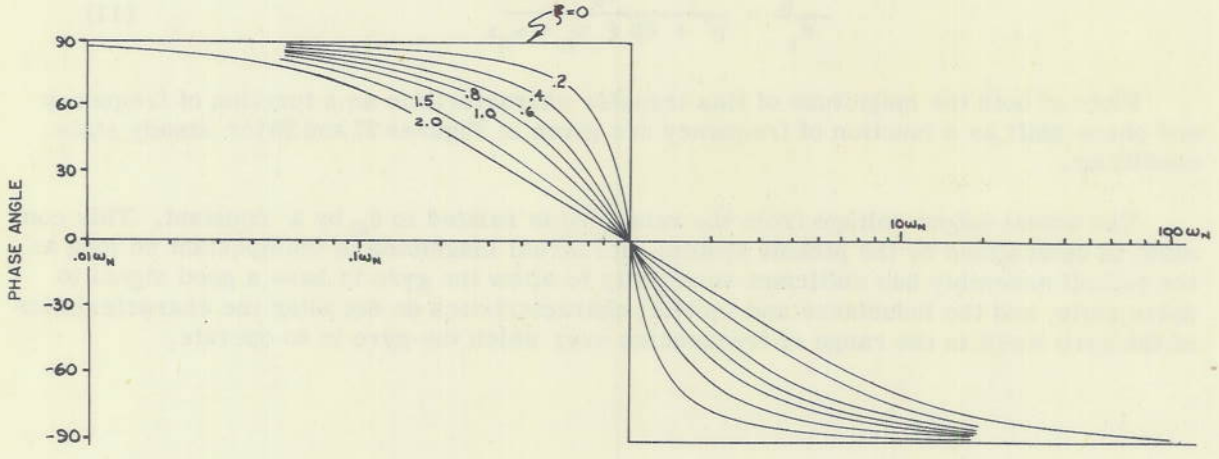

Figure 28

APPENDIX II

Airframe Characteristic

No discussion of autopilot characteristics would be complete without analysis of the loop with the exact expression for the airframe transfer characteristic.

In the body of this report, it was assumed that the transfer characteristic of the airframe, from flap motion to missile motion is:

$$\frac{\Phi}{\delta_f} = \frac{\omega_a}{p} \tag{1}$$

A more exact solution for this transfer characteristic has been obtained, using the method developed in another report.* It is:

$$\frac{\Phi}{\delta_f} = \frac{1 + \frac{p}{\omega_{15}}}{\frac{p}{\omega_{16}}\left(Ap^2 + Bp + 1\right)} \tag{2}$$

where

$$\omega_{16} = \frac{qS}{mV}\left[\frac{C_{m\alpha}\, C_{l\delta} - C_{m\delta}\, C_{l\alpha}}{\frac{qS}{mV}\, C_{mq}\, C_{l\alpha} + C_{m\alpha}}\right]$$

$$\omega_{15} = \frac{qS}{mV}\left[\frac{C_{m\alpha}\, C_{l\delta} - C_{m\delta}\, C_{l\alpha}}{C_{m\delta}}\right]$$

$$A = \frac{1}{\frac{qSc}{I}}\,\frac{-1}{\left[\frac{qS}{mV}\, C_{mq}\, C_{l\alpha} + C_{m\alpha}\right]}$$

$$B = A\left[\frac{qS}{mV}\, C_{l\alpha} - \frac{qSc}{I}\, C_{mq}\right]$$

The notation and sign convention used is that of the NACA. These equations show that the limiting cases will be as follows:

(a) Sea level, minimum weight, high speed condition, which yields $\omega_{15} = 5.30$ rad/sec; $\omega_{16} = .524$ rad/sec; $A = .0188$ sec^2/rad^2 $B = .1005$ sec/rad.

(b) High altitude, maximum weight, low speed conditions, which yields $\omega_{15} = 1.40$ rad/sec; $\omega_{16} = .0602$ rad/sec; $A = .0943$ sec^2/rad^2; $B = .0681$ sec/rad.

Figures 29 and 30 show plots of the transfer characteristic, both amplitude and phase, for these conditions.

In an exact solution for this problem an additional term in the closed loop must be included to compensate for the effect of the flap servo. The flap servo is linear out to a

---

* NRL Report R-3253, Response of an Airframe to Sinusoidal Wing Flap Deflection, by James W. Titus, Radio Div. III, NRL.

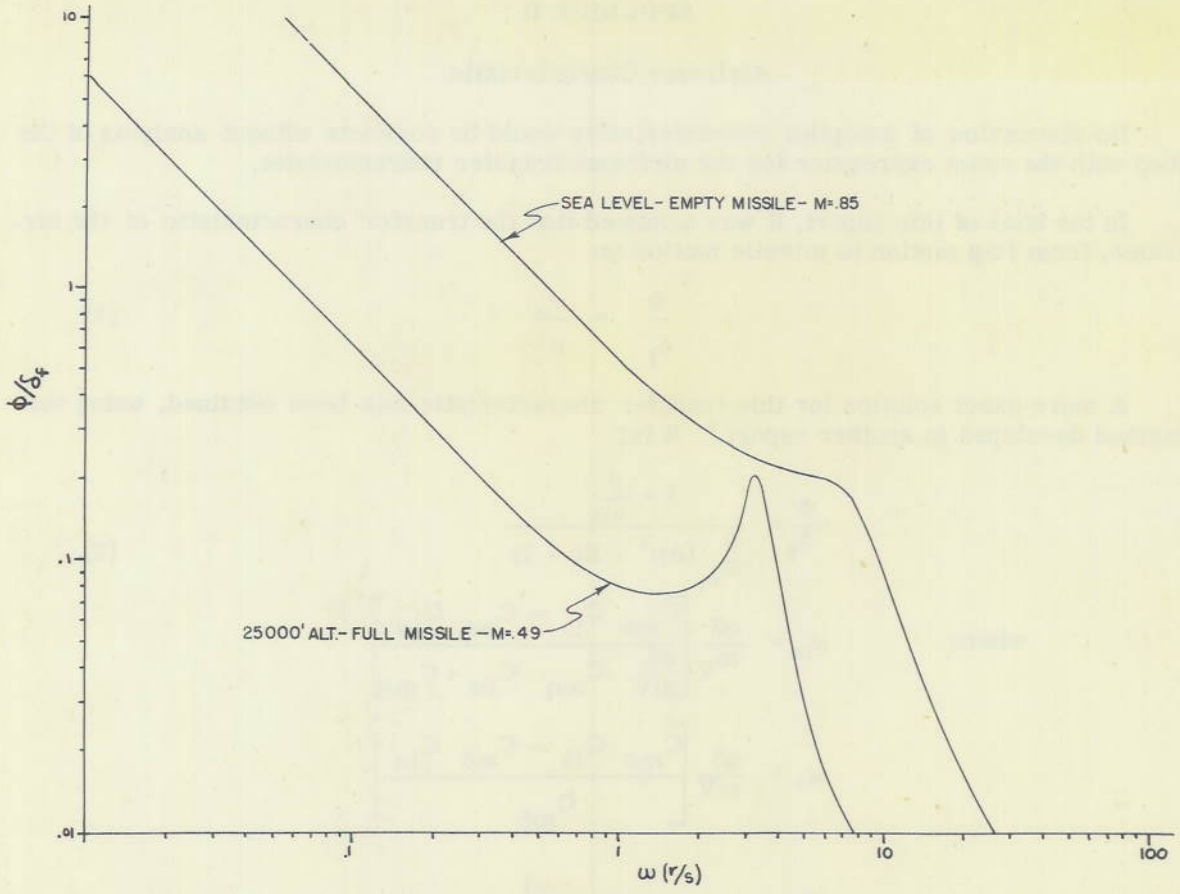

Figure 29

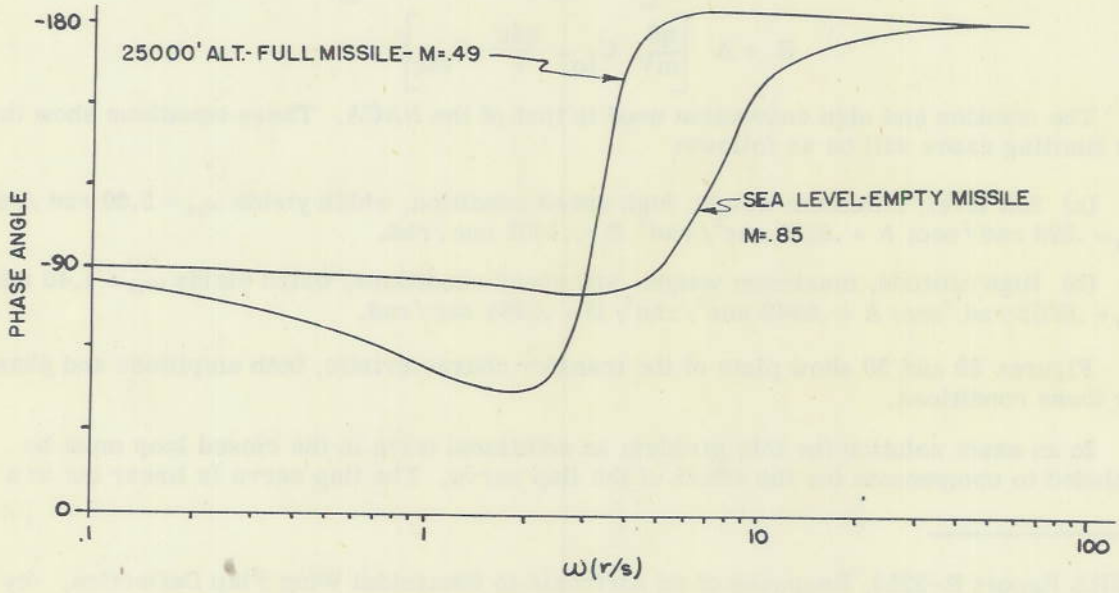

Figure 30

frequency which we shall adjust to be $10\omega_f$. The will cause the open loop transfer characteristic of the autopilot, flap servo, and airframe characteristics to be

$$\mu_5 = \left(\frac{p}{\omega_a}\right)\left(\frac{\omega_f}{p}\right)\left(\frac{\omega_f + p}{\omega_f}\right)\left(\frac{10\,\omega_f}{10\,\omega_f + p}\right)\left(\frac{\omega_{15} + p}{\omega_{15}}\right)\left(\frac{\omega_{16}}{p}\right)\left(\frac{1}{Ap^2 + Bp + 1}\right) \tag{3}$$

If we adjust the constants involved so that

$$\omega_f = 3.16$$

$$\frac{k\,\omega_f}{\omega_a} = 40$$

and substitute the airframe characteristics for the two missile operating conditions, we obtain the transfer characteristics for μ_5 shown in Figures 31 and 32. The open loop phase shifts at $\mu_5 = 1$, or gain crossover, for case (a) is -147^0, and for case (b) of -130^0, both of

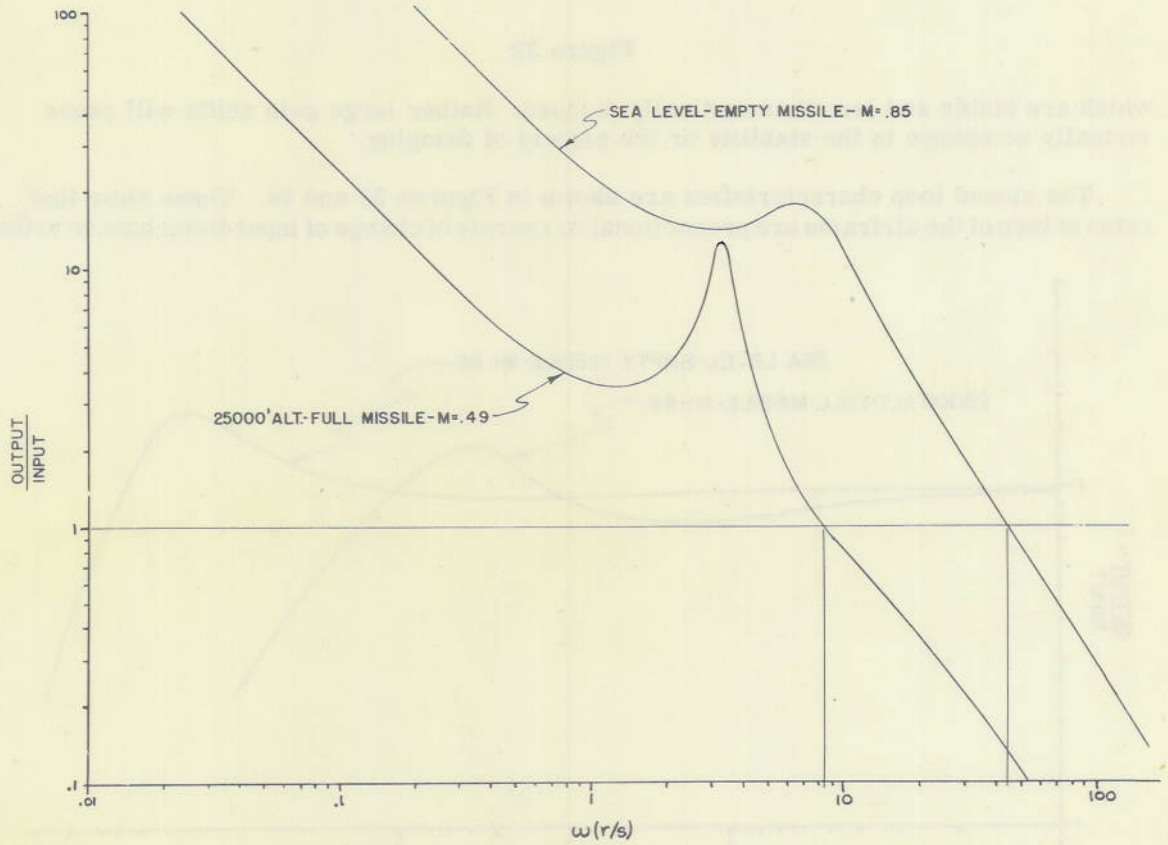

Figure 31

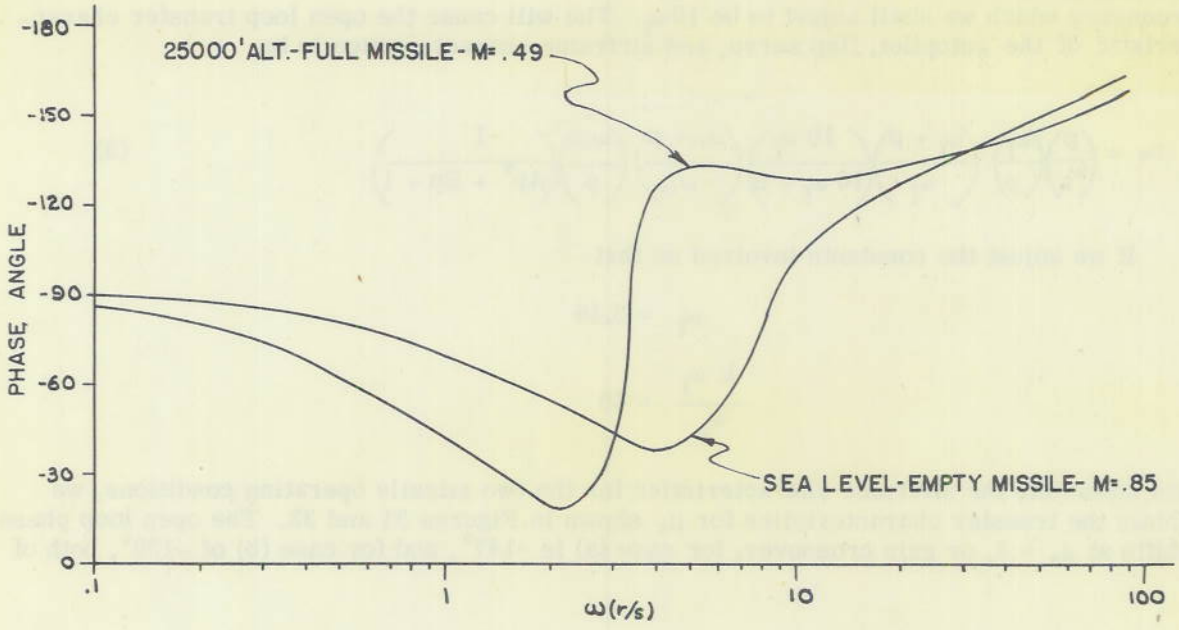

Figure 32

which are stable and less than critically damped. Rather large gain shifts will cause virtually no change in the stability or the amount of damping.

The closed loop characteristics are shown in Figures 33 and 34. These show that rates of turn of the airframe are proportional to the rate of change of input disturbances to the

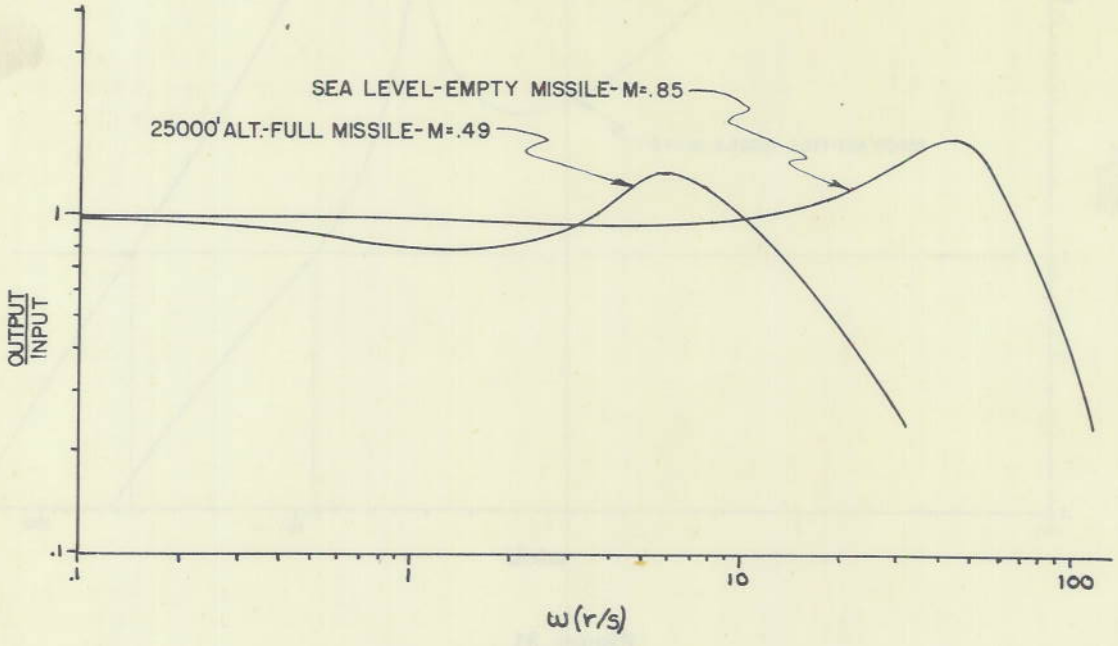

Figure 33

airframe, and that the angle of the airframe is the integral of an input control signal to the autopilot, considering that part of the closed loop is the rate gyro feedback. Hence, the criterion originally set up, that is, that the missile-autopilot combination act as an integrator of input control signals, is fulfilled.

These results will not be affected by an angle of attack control system if that system is designed to have a very narrow bandpass, that is, it operates merely to reduce zero frequency drift. This is the only requirement placed on the angle of attack system by this analysis.

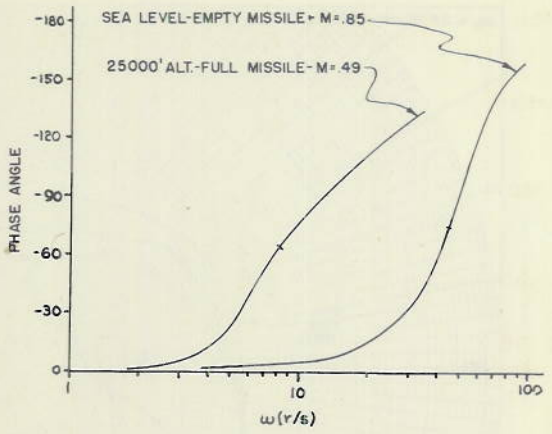

Figure 34

APPENDIX III

Rate Gyro Selection

In stability studies of a system it is necessary to investigate the phase and gain margins of the open loop transfer characteristics. This may be done by using graphs of phase and gain plotted against frequency or may be done using Nyquist diagrams, a combination of these two, as is done in this case for study of the effect of variation of gyro resonant frequency and damping on the stability of the airframe-autopilot loop.

Figures 35, 36, 37, 38, and 39 show Nyquist diagrams for the loop under various conditions. In Appendix II the open loop airframe-autopilot characteristic was developed, using an approximation for the rate gyro. The actual performance of the loop combining these results with the true gyro characteristics studied in Appendix I is carried out.

Figure 35 shows the results with the gyro resonant frequency ω_n = 25 radians per second, with various damping ratios ξ. The maximum resonant frequency case is that obtained when the airframe has a velocity corresponding to M = .85, at sea level and empty. The minimum resonant frequency case is assumed as M = .49, full missile at 25000 feet altitude. With ω_n 25 radians per second the minimum resonant frequency case is stable but the maximum resonant frequency case encircles the (-1, 0) point and is unstable.

Figures 36 and 37 show the system at higher values of ω_n. These show improvement but are unstable.

Figure 38, where the resonant frequency ω_n is 150 radians per second is stable for all conditions of the Skylark airframe but shows only small phase and gain margins for the high resonant frequency case.

Figure 39, ω_n = 200 radians per second shows adequate phase margins and gain margin for the damping values shown. Hence it follows that the resonant frequency of the gyro for the Skylark autopilot should be of the order of 200 radians per second.

Although the damping ratio ξ has little affect on stability, the bandpass is materially effected by changes in this factor. The susceptibility to noise makes it desirable to exclude low damping ratios from consideration. High damping ratios are excluded by bandpass considerations. A damping ratio of ξ = .4 to .65 represents a reasonable range of values.

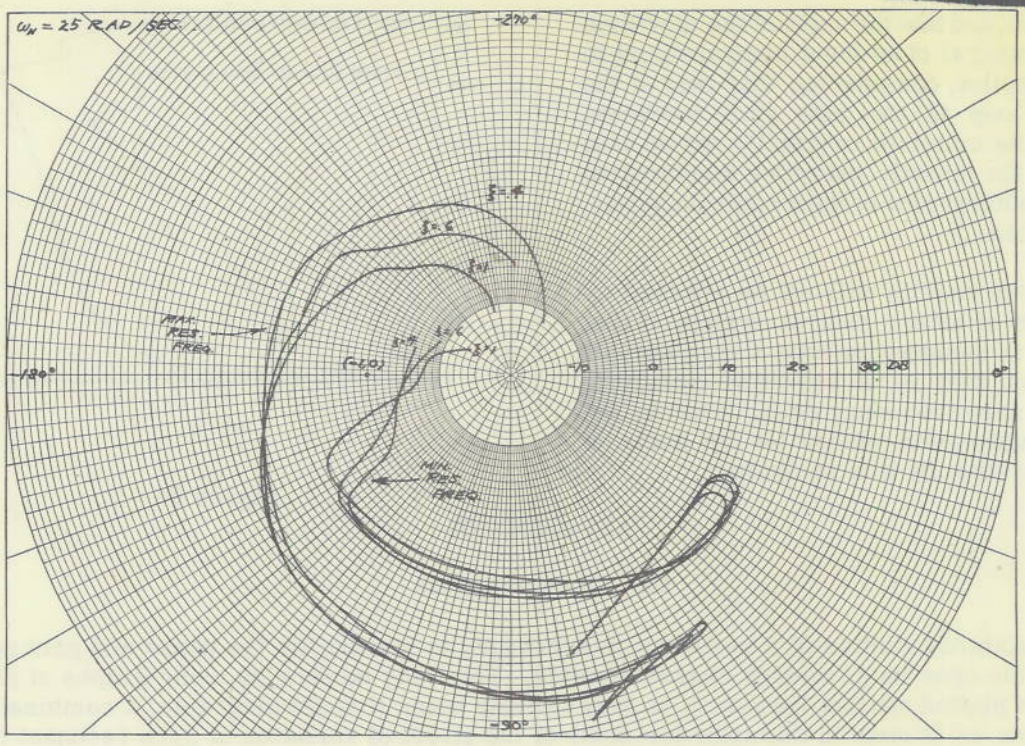

Figure 35

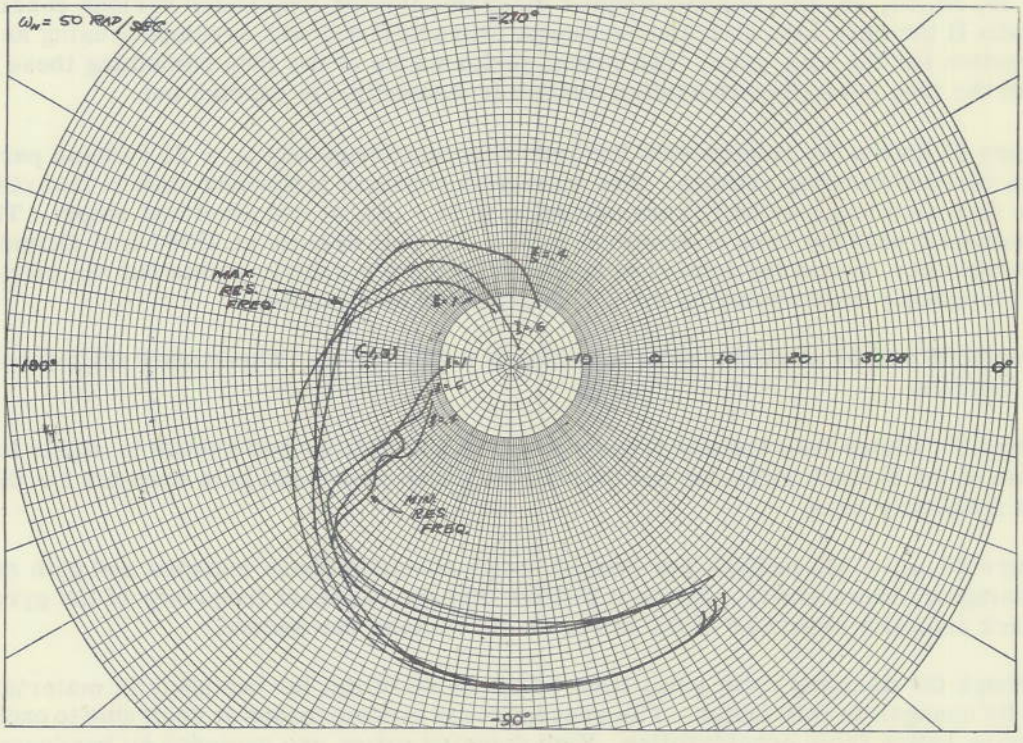

Figure 36

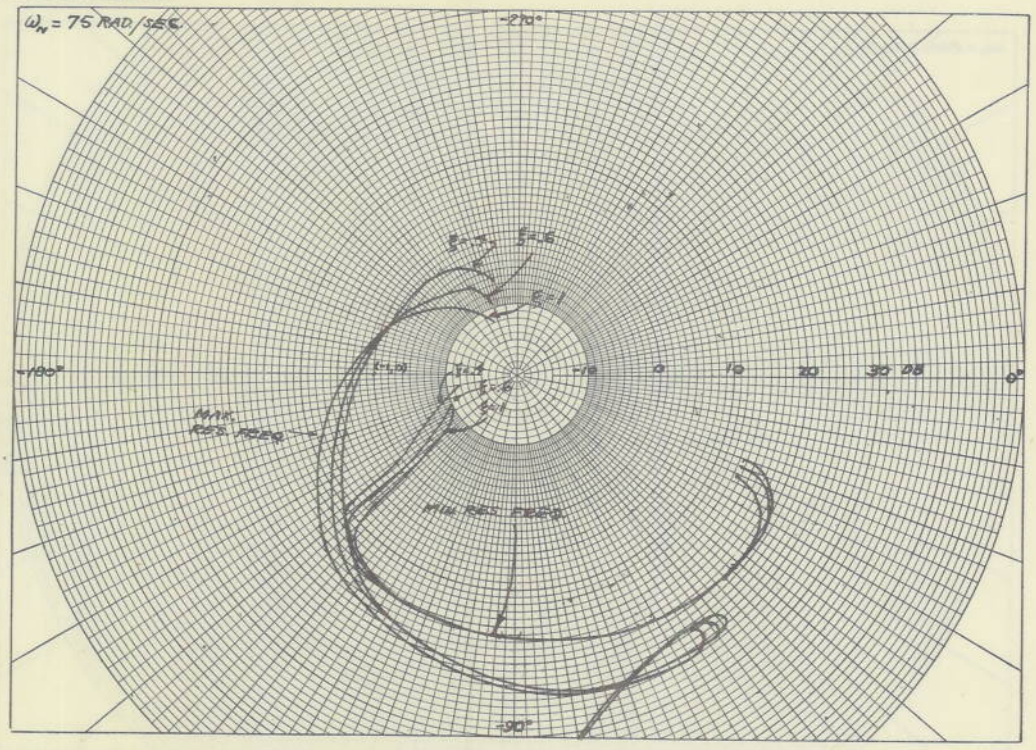

Figure 37

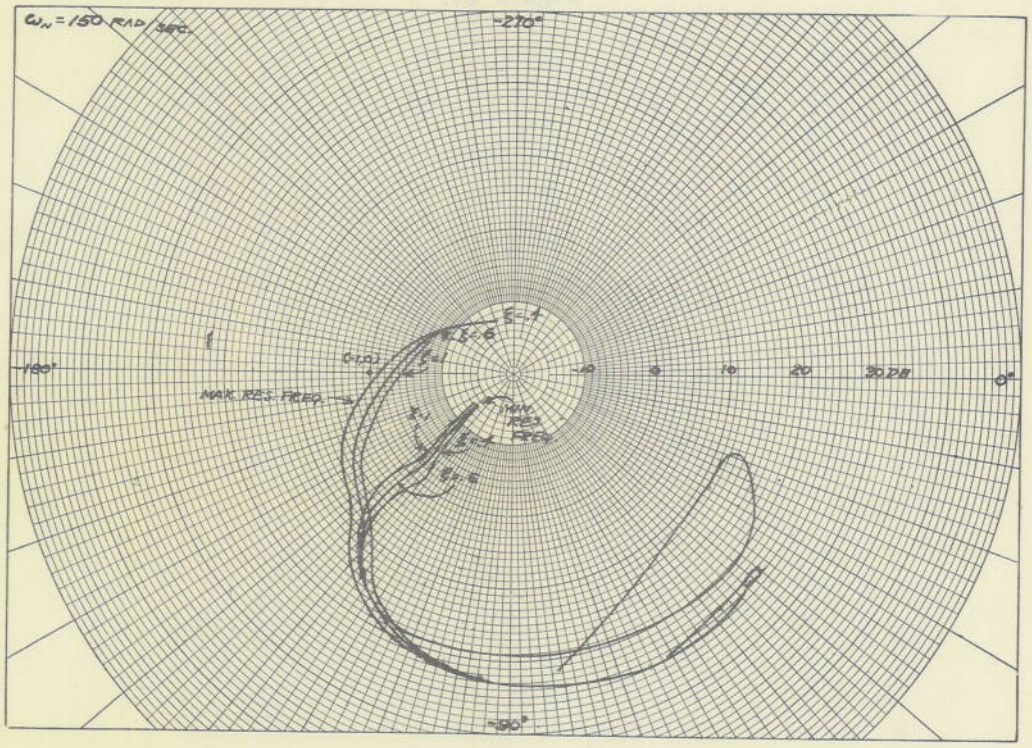

Figure 38

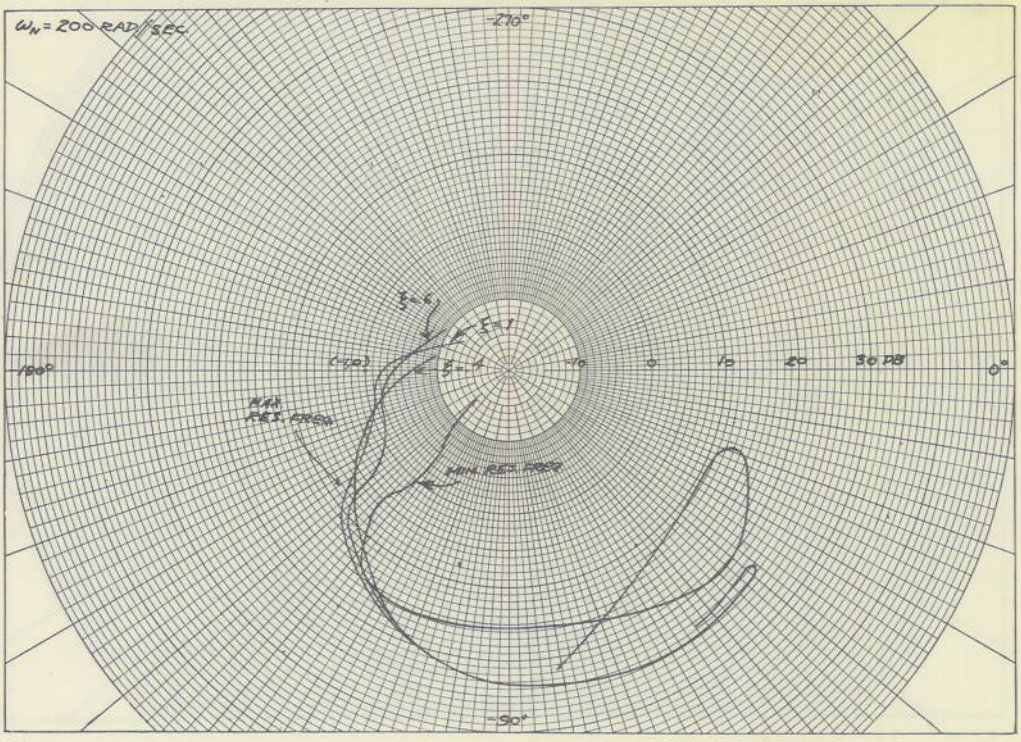

Figure 39